CT-923-SS1
DON. 7016

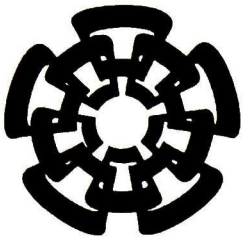

Centro de Investigación y de Estudios Avanzados
del Instituto Politécnico Nacional
Unidad Guadalajara

Extracción automática de pixeles puros para el análisis de imágenes hiperespectrales.

Tesis que presenta:
Jairo Salazar Vázquez

para obtener el grado de:
Maestro en Ciencias

en la especialidad de:
Ingeniería Eléctrica

Director de Tesis
Dr. Andrés Méndez Vázquez

CINVESTAV del IPN Unidad Guadalajara, Guadalajara, Jalisco, Agosto de 2015.

Extracción automática de pixeles puros para el análisis de imágenes hiperespectrales.

Tesis de Maestría en Ciencias
Ingeniería Eléctrica

Por:
Jairo Salazar Vázquez
Licenciado en Sistemas de Información
Universidad de Guadalajara 2003-2005

Becario de Conacyt, expediente no. 369844

Director de Tesis
Dr. Andrés Méndez Vázquez

CINVESTAV del IPN Unidad Guadalajara, Agosto de 2015.

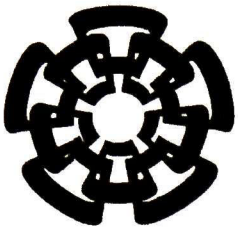

Centro de Investigación y de Estudios Avanzados

del Instituto Politécnico Nacional

Unidad Guadalajara

Automatic endmember extraction algorithms for hyperspectral image analysis

A thesis presented by·

Jairo Salazar Vázquez

to obtain the degree of:

Master in Science

in the subject of:

Electrical Engineering

Thesis Advisors:

Dr. Andrés Méndez Vázquez

CINVESTAV del IPN Unidad Guadalajara,Guadalajara, Jalisco, August, 2015.

Declaration of Authorship

I, Jairo Salazar Vázquez., declare that this thesis titled, 'Automatic endmember extraction algorithms for hyperspectral image analysis.' and the work presented in it are my own. I confirm that:

- This work was done wholly or mainly while in candidature for a research degree at this University.
- Where any part of this thesis has previously been submitted for a degree or any other qualification at this University or any other institution, this has been clearly stated.
- Where I have consulted the published work of others, this is always clearly attributed.
- Where I have quoted from the work of others, the source is always given. With the exception of such quotations, this thesis is entirely my own work.
- I have acknowledged all main sources of help.
- Where the thesis is based on work done by myself jointly with others, I have made clear exactly what was done by others and what I have contributed myself.

Signed: 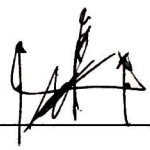

Date: 03-08-2015

Dedicated to all people who motivated me along my life to obtain the master in science degree.

Jairo Salazar Vázquez.

Resumen

CENTRO DE INVESTIGACIÓN Y ESTUDIOS AVANZADOS DEL INSTITUTO POLITÉCNICO NACIONAL

Departamento de Ingeniería Eléctrica

Maestría en ciencias

Extracción automática de pixeles puros para analizar imágenes hiperespectrales.

por Jairo Salazar Vázquez.

Debido a que las imágenes hiperespectrales tienen una alta resolución espectral, han permitido desarrollar algoritmos para detectar objetos y generar mapas de distribución de materiales en un área geográfica para aplicaciones de agricultura, seguridad y defensa, industria, etc., como Dimitris [Dimitris, 2002] comentó: "*explotando el hecho de que diferentes materiales refractan, absorben y emiten energía electromagnética, de forma distinta en cada longitud de onda, definiendo patrones identificables debido a su composición molecular*" En esta tesis se explora la idea de extraer los endmembers de una imagen hiperespectral de forma automática y sin requerir parámetro alguno. Como resultado de la investigación, se propone el algoritmo FuzzyVD para estimar el número de endmembers presentes en una imagen hiperespectral y también se propone el algoritmo SMV$\perp$ para extraer un número dado de endmembers de dicha imagen. Al utilizar FuzzyVD y SMV$\perp$ en conjunto, es posible realizar el proceso de extracción de endmembers sin necesidad de parámetros o entrenamiento. El desempeño de los algoritmos propuestos ha sido comparado con los algorimos similares encontrados en la literatura de identificación de endmembers y los resultados permiten concluir que tanto FuzzyVD como SMV$\perp$ son robustos y confiables.

Abstract

CENTRO DE INVESTIGACIÓN Y ESTUDIOS AVANZADOS DEL INSTITUTO POLITÉCNICO NACIONAL
Electrical Engineering Department

Master in Science

Automatic endmember extraction algorithms for hyperspectral image analysis.

by Jairo Salazar Vázquez.

The high spectral resolution of the Hyperspectral Images (HI) allows to develop different algorithms for target detection, material mapping, and material identification. This has applications in agriculture, security, industry, and defense [Dimintris, 2002] "*by exploiting the fact that different materials reflect, absorb, and emit electromagnetic energy, at specific wavelengths, in distinctive patterns related to their molecular composition*" This thesis explores the idea of extracting the endmembers present in a hyperspectral image using a totally automatically approach without parameter settings. As a result, the FuzzyVD algorithm is proposed in order to estimate the number of endmembers present in a given hyperspectral image and the SMV$\perp$ algorithm is proposed for endmembers extraction. The combination of both algorithms enables the endmember extraction process in a non-supervised way. The performance of SMV$\perp$ and FuzzyVD in synthetic and real hyperspectral images have been compared against several of the state of the art algorithms with similar features through the literature of endmember identification, and the results allow to conclude that the proposal is robust and reliable.

Acknowledgements

To my mother who supported me since the beginning of my studies.

To my father that taught me to work.

To Nancy who supported me and encouraged me since PADTS.

To my advisor Dr. Andrés Méndez who motivated me, guided me, and supported me throughout the research.

To Dr. Raúl Gonzales, Dr. Ernesto López, Dr. Mario Siller, and Dr. Féliz Ramos for the knowledge that they gave me.

To my classmates: Armando, Arturo, Rubén, Mario, Ivan, and Edith who supported me in the learning process and they allowed me to enjoy the postgraduate studies.

To Dr. Cuauhtemoc López who taught me how to select my thesis topic.

To M.C. Cacama Solís Peñafiel who is the first person to told me about the CINVESTAV.

To all people who influenced me to study postgrade.

To CONACYT and especially to the Mexican citizens for the economic support.

Contents

List of Figures

List of Tables

Abbreviations

ATGP	**A**utomatic **T**arget **G**eneration **P**roccess
AVIRIS	**A**irborne **V**isible / **I**nfra**R**ed **I**maging **S**pectrometer
AWGN	**A**dditive **W**hite **G**aussian **N**oise
CMER	**C**lustering **M**ethod based upon **E**quivalence **R**elations
EEA	**E**ndmember **E**xtraction **A**lgorithms
HI	**H**yperspectral **I**mage
HFC	**H**arsanyi **F**errand **C**hang
HSI	**H**yperspectral **I**maging **S**ensors
LMM	**L**inear **M**ixing **M**odels
MNF	**M**aximum **N**oise **F**raction
NAPC	**N**oise **A**djusted **P**rincipal **C**omponents
NWHFC	**N**oise **W**hitened **H**arsanyi **F**errand **C**hang
OBA	**O**rthogonal **B**ases **A**proach
PPI	**P**ixel **P**urity **I**ndex
SGA	**S**implex **G**rowing **A**lgorithm
SMV$\perp$	**S**implex of **M**aximal **V**olume using **P**erpendicular altitude
TEP	**T**hreshold **E**nergy **P**ercentage
USGS	**U**nited **S**tates **G**eological **S**urvey
VD	**V**irtual **D**imensionality

Symbols

$\oplus$	:= XOR operation.
$\mathbb{N}$	:= $\{1, 2, 3, ...\}$.
$\mathbb{R}$	:= The set of all real numbers.
$\mathbb{K}$	:= A field.
$[a, b], (a, b], [a, b), (a, b)$	:= Closed, left-open, right-open, open interval or real numbers between a and b, respectively.
$\mid x \mid$	:= Absolute value of x.
$\vec{u}$	:= u is a vector.
$\langle \vec{u}, \vec{v} \rangle$	:= Dot product of the vectors $\vec{u}$ and $\vec{v}$.
$\parallel \vec{u} \parallel$	:= $\sqrt{\langle \vec{u}, \vec{u} \rangle}$.
$!$	:= Factorial.
$A \setminus B$	:= Set A minus set B.
$\{\emptyset\}$	:= Empty set.
$\in$	:= Is an element of.
$\notin$	:= Is not an element of.
$\cup, \cap$	:= Set union and set intersection respectively.
$\subset, \subseteq$	:= Proper subset of and subset of respectively.
$\vec{u}^{\perp}$	:= Orthogonal complement of $\vec{u}$.
$\wp$	:= Power set.
$\#A$	:= Cardinality of the set A.
ξ	:= The collection of all subsets $E \in \wp$, such that $\#E = k$, for a given $k \in \mathbb{N}$.
$\circ$	:= Composition of relations or functions.
${}^{\alpha}A, {}^{+\alpha}A$	:= Alpha cut and strong Alpha cut respectively.
σ^2	:= Sample standard deviation.

Chapter 1

Introduction

This chapter provides an overview about the hyperspectral image analysis, their applications and previously works developed on this research field. Afterwards, it gives a description of the main problem studied in this thesis, and the motivation to propose new solutions for the problem.

1.1 Background

A Hyperspectral Image (HI) is a set of two dimensional digital images acquired simultaneously from a physical surface where each image express the electromagnetic energy sensed at a specific wavelength. Typically, they are in the spectrum range of 0.4-2.5μm with continuous and narrow separation of 0.004-0.01μm. Given that each image in the HI has the same area, each pixel represents exactly the same spatial area that the same pixel in the other images.

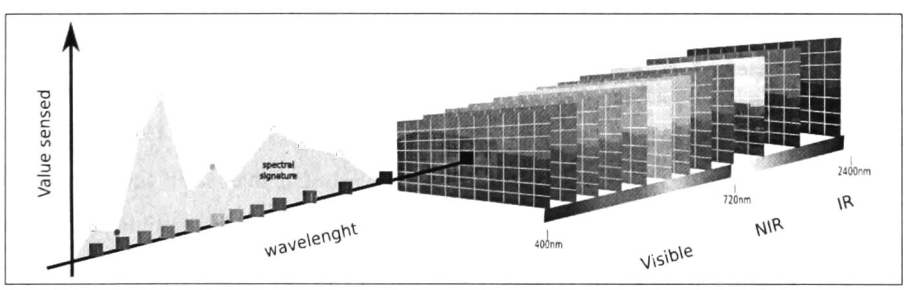

FIGURE 1.1: A hyperspectral image. Redrawn from [21].

The application fields of hyperspectral image analysis has been increasing in the last years because the availability of new devices for hyperspectral image acquisition and public hyperspectral datasets (e.g. AVIRIS[1] or USGS[2]). The high spectral resolution of these images, allows to develop different algorithms for target detection, material mapping, and material identification for applications in Agriculture [3], Security and Defense [3], Industry [3], etc.

In some applications, it is possible to perform target detection and material mapping, measuring in laboratory the light refraction, light emission, and light abortion at different wavelengths that each material of interest generates, identifying its specific pattern or *spectral signature* (Definition 3).

However, for many other applications, there is not enough available prior information, or spectral signatures. For example, in many applications of remote sensing or precision agriculture, material distribution is required to obtain a correct classification of the pixels present in the HI. For this type of applications, it is necessary to decompose the scene in the respective *abundances composition of the pure spectral signatures, or the constituent spectral, referred to as* ***endmembers*** [4]. For this type of applications, it is possible to summarize the hyperspectral image analysis process as follows: estimate the total number of endmembers present in the HI, identify the endmember pixels, and unmix the original scene using the set of endmembers extracted in order to be able to target detection, target identification and material mapping. It is possible to estimate the number of endmembers present in the HI using the HFC [5], NWHFC [5], or TEP [6] algorithms. In order to identify the set of endmembers, the Endmember Extraction Algorithms (EEAs) use Statistical Methods (SM) [7], Orthogonal Subspace Projections (OSP) [6], Linear Mixing Models (LMM) [8], etc., there are several EEAs (e.g. N-FINDR [8], SGA[9], PPI[10], OBA [11], ATGP [16], and others). One of the most used technique by the EEAs is the LMM because the convex nature of the hyperspectral dataset and the spatial resolution. This type of algorithms search the set of spectral pixels that inscribe the simplex [12] of maximal volume, by assuming that all of them are endmembers and the remainder *spectral pixels* (Definition 2) are linear combination of them [8]. The (Figure 1.2) provides fourth different simplexes. Finally, the unmixing processes can be performed using the methods proposed by *Winter* [8], the procedure proposed by *Tao*

et al. [11], etc.

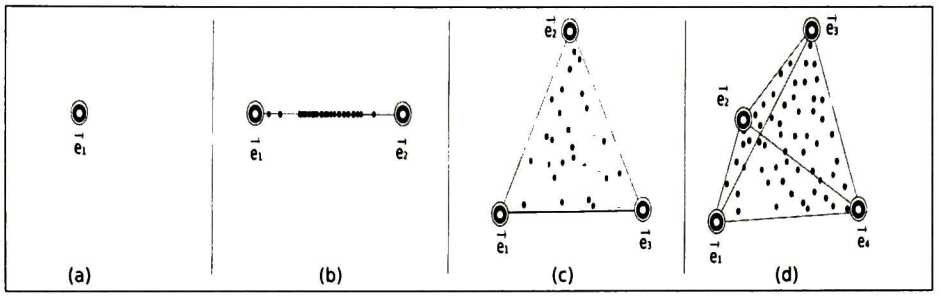

FIGURE 1.2: (a-d) Simplex of maximal volume in $\mathbb{R}^0$, $\mathbb{R}^1$, $\mathbb{R}^2$, and $\mathbb{R}^3$ respectively.

The present thesis explores the idea of building a deterministic method to estimate the simplex of maximal volume using a bottom-up approach by taking advantage of the LMM assumptions. As a result, the proposed algorithm SMV⊥ is based on the use of orthogonal complements [12] and the Gram-Schmidt process [13]. In order to prove its efficiency, SVM⊥ has been compared against N-FINDR, ATGP and OBA because they are the algorithms that show the greatest similarity to SMV⊥ through the literature of endmember identification. The measurements used for comparison were the *computational time complexity*, *execution time*, and *the final volume of the simplex in* $\mathbb{R}^n$ This is due to their accuracy to evaluate the performance of the algorithms for LMM. Furthermore, many EEAs including SMV⊥, require to estimate previously the number of endmembers to be extracted. In this thesis is proposed the FuzzyVD algorithm to estimate the number of endmembers present in a hyperspectral image. FuzzyVD facilitates the hyperspectral image analysis process because it does not require threshold setting, prior information, noise removal, dimensional reduction, low information band removal, water absorption band removal nor calculating the eigenvalues [14]. In order to do this, FuzzyVD exploits the properties of the SMV⊥ algorithm, fuzzy equivalence relations [15], fuzzy Minkowski distance[15], fuzzy logic [15] and fuzzy systems [15], improving the reliability of the methods currently present in the literature, avoiding the threshold setting (estimate this, some times is as difficult as estimate the number of endmembers present in the HI), and expands the application field of fuzzy logic and fuzzy systems into the hyperspectral images analysis. FuzzyVD also provides a method to design fuzzy systems to define a total order in a set of possible partitions when desirable characteristics are well known. This algorithm has been applied to real

AVIRIS [1] images (Cuprite, Nevada) and synthetic hyperspectral imagery proposed by Chang in [16]. Finally, a comparative analysis about FuzzyVD, HFC, NWHFC, and TEP performance is given.

1.2 Motivation

The Hyperspectral Imaging Sensors (HSI) are a relatively new technology, nevertheless, their use have been increasing in the recent years because them enable the target detection and identification. Due to their high spectral resolution, the HIs can be considered Big data [17] requiring the correct data structures and algorithms to obtain the optimal results in acceptable time.

Moreover, due to there are many HI applications (e.g. New planets exploration, Remote Sensing, Materials mapping, etc.) where no prior information exists and it is not possible execute a training phase for classification algorithms, the HI analysis is a new area of research for the non-supervised and semi-supervised [18] machine learning algorithms.

Furthermore, by studying the state of the art, it has been found many opportunities in the hyperspectral data analysis for new and improved algorithms.

1.3 Problem Description

One of the most representative EEAs based on the LMM, is probably the N-FINDR because it is easy to understand and implement, a mayor drawback of N-FINDR is its high computational complexity because its combinatorial nature. In addition, the final results given by N-FINDR are highly dependent on a random initialization. Because of all these reasons, different versions of this algorithm have been developed (e.g. SGA [9], SM N-FINDR [19], SQ N-FINDR [19], SC N-FINDR [19], IN-FINDR [19], etc.) in order to try to overcome these disadvantages. Although these algorithms mitigate the N-FINDR's disadvantages, they still perform the calculation of a matrix determinant several times even when a single pixel is evaluated at each iteration. Furthermore, the

possible solutions are restricted by the volume of the subspace spanned by the remainder non-valuated candidates. Therefore, it is necessary to improve the performance of these algorithms in order to reduce the computational complexity for the endmember extraction phase of the HI analysis.

Moreover, due to the fact that many EEAs require to estimate the number of different endmembers present in a HI in advance, it is necessary to have a robust method to estimate such an important initialization parameter. There are different algorithms able to estimate this parameter and many of them are based on eigenvalues. Nevertheless, for many applications these algorithms are unable to provide dependable results. Then, it is necessary to explore different approaches in order to develop algorithms with greater performance than the existing ones.

1.4 Goals

1.4.1 General Goal

The main aim of this thesis is to develop robust algorithms for endmember extraction, and for the correct estimation of the number of endmembers present in a HI using the Gram-Schmidt orthogonalization process, fuzzy relations, and adequate data structures in order to exceed the results obtained by the classic algorithms present in the literature.

1.4.2 Specific Goals

1. Reduce the complexity of the N-FINDR by implementing a bottom-up approach using orthogonal complements.
2. Develop deterministic methods to avoid the undesired non-deterministic characteristic of the N-FINDR algorithm.
3. Exploit the Fuzzy Logic's capability to formalize the intuitive reasoning and the non-supervised crisp partition specification, in order to develop an algorithm to estimate the number of endmembers present in a HI.

4. Explore the idea of develop a total non-supervised algorithm for fast endmember extraction that does not require any parameter or prior information.

1.5 Original Contributions

1. Two novel non-supervised algorithms were developed:
   (a) The SMV⊥ which calculates the set of vectors that inscribe the simplex (Geometrical object: Definition 8) of maximum volume in $\mathbb{R}^n$ for a dataset of n dimensions. This algorithm has been applied for fast endmember extraction in synthetic and real hyperspectral images. A great advantage of the proposed algorithm is its low time complexity $O(n)$ with n the number of pixels.
   (b) FuzzyVD which estimates the number of different endmembers present in a HI based on fuzzy systems, Gram-Schmidt orthogonalization process, and statistical methods.
2. The fuzzy systems application field was expanded into HI analysis because it was not possible to find any other previous research work where the fuzzy system was applied to estimate the number of endmembers present in a HI.
3. A novel method was introduced to define a total order in a set of possible partitions when desirable characteristics are well known.

1.6 Document Organization

The remainder of this document is organized as follows: **Chapter** 2 gives a theoretical background to support the understanding of this thesis. **Chapter** 3 introduces the approaches typically used for endmember extraction, and to estimate the number of endmembers present in a HI. **Chapter** 4 introduces a detailed description of the SMV⊥ algorithm proposed for endmember extraction, and the FuzzyVD algorithm proposed to estimate the number of endmembers present in a HI. **Chapter** 5 provides the steps used to obtain the hyperspectral images used in the experiments, it describes the experiments performed, and it shows a comparative analysis of the results obtained by the proposed

algorithms against related algorithms. **Chapter** 6 gives a conclusion and it proposes forthcoming research. Finally, the **Bibliography** and the **Releases** published during the research are attached.

This page is intentionally left blank.

Chapter 2

Theoretical Framework

In this chapter a theoretical background is given in order to support the understanding of the algorithms proposed.

2.1 Hyperspectral Images

The definitions of *hyperspectral image* and *spectral pixel* are introduced in order to provide a convenient representation of these two important and widely used concepts during all phases of the algorithms proposed in this thesis.

Definition 1. A **hyperspectral image** is a three dimensional matrix $P \in \mathbb{K}^{R \times C \times L}$ where $\mathbb{K}$ is a field; R, C and L are the total number of rows, columns and layers respectively.

Thus, it is possible to define what is a spectral pixel.

Definition 2. Let P be a hyperspectral image then, a **spectral pixel** is a vector $\vec{p}$ such that:

$$\vec{p} = \{P_{r,c,1}, P_{r,c,2}, ..., P_{r,c,L}\} \tag{2.1}$$

where $1 \leq r \leq R$ and $1 \leq c \leq C$, and $R, C \in \mathbb{N}$.

For convenience at the computing time, any hyperspectral image P (with R rows, C columns and L layers) is represented using a two dimensions matrix $X \in \mathbb{K}^{L \times N}$ where $\mathbb{K}$ is a field, L is the number of layers and N is the total number of spectral pixels in P respectively, such that

$$N = R \times C, \tag{2.2}$$

and

$$[X_{1,i}, X_{2,i}, ..., X_{L,i}] = \vec{x}_i = \vec{p}_i = [P_{r,c,1}, P_{r,c,2}, ..., P_{r,c,L}], \tag{2.3}$$

for all $\vec{x}_i \in X$ and each $\vec{p}_i \in P$: $1 \leq i \leq N$ and i is calculated using (Equation 2.4)

$$i = ((r-1) \times C) + c. \tag{2.4}$$

Because the value sensed by a HSI at each wavelength for a given pixel in a HI depends on the type of material located in the area of the scene represented by that pixel, it is possible to say that every pixel has a characteristic signature related. That signature is known as *spectral signature* and is defined as follows.

Definition 3. A **spectral signature** is a pattern related to a specific *spectral pixel.*

Although the LMM is a well known and often used model for the HI analysis, in this thesis is presented a detailed description of this model in (Section 3.1.1). Assuming that the LMM is a good approximation, there are pure *spectral pixels* located in a given HI. Pure in the sense that, the spectral signature corresponds to only one type of material. The pure spectral pixels are referred as endmember and it is defined as follows.

Definition 4. An **endmember** is the assumption that there exists at less one pure spectral pixel in a hyperspectral image where the spectral signature belongs to only one type of material.

Once defined the endmember, it is possible to establish that every one *distinct signal* [14] in a HI is an endmember for the LMM. This important remark is used in the following definition, in order to provides a practical notion of this important concept.

Definition 5. The Virtual Dimensionality (**VD**), is the total number of different signals present in a hyperspectral image and every different signal is an endmember.

2.2 Simplex

The (Theorem 1) allows to infer that the maximum number of endmembers present in a given hyperspectral image X, are at most equal to the number of dimensions of X.

Theorem 1 ([12]). Suppose that $\vec{x}_1, \vec{x}_2, ..., \vec{x}_n$ span a linear space X, and the vectors $\vec{y}_1, \vec{y}_2, ..., \vec{y}_j \in X$ are linear independent then, $j \leq n$.

Proof.[12] Since $\vec{x}_1, \vec{x}_2, ..., \vec{x}_n$ span X, every vector in X can be written as a linear combination of $\vec{x}_1, \vec{x}_2, ..., \vec{x}_n$. In particular, $\vec{y}_1$:

$$\vec{y}_1 = k_1\vec{x}_1 + k_2\vec{x}_2 + ... + k_n\vec{x}_n \tag{2.5}$$

Since $\vec{y}_1 \neq 0$ not all k, are equal to 0, say $k_i \neq 0$. Then $\vec{x}_i$ can be expressed as a linear combination of $\vec{y}_1$ and the remainder $\vec{x}_s$. So the set consisting of the $\vec{x}'s$, with $\vec{x}_i$ replaced by $\vec{y}_1$ span X. If $j \geq n$, repeat this step $n-1$ more times and conclude that $\vec{y}_1, \vec{y}_2, ..., \vec{y}_n$ span X: if $j > n$, this contradicts the linear independence of the $\vec{y}'s$ for then $\vec{y}_{n+1}$ is a linear combination of $\vec{y}_1, \vec{y}_2, ..., \vec{y}_n$. □

The following definition is used to calculate the distance between any vertex $\vec{x} \in X$, and the subspace spanned by a base of endmembers.

Definition 6 ([12]). Let X be a finite-dimensionality linear space with Euclidean structure, Y a linear subspace of X. The **orthogonal complement** of Y, denoted as $Y^{\perp}$, consists of all vectors $\vec{z} \in X$ that are orthogonal to every $\vec{y} \in Y$:

$$\vec{z} \in Y^{\perp} \quad \text{iff} \quad \langle \vec{y}, \vec{z} \rangle = 0 \qquad \text{for all} \quad \vec{y} \in Y \tag{2.6}$$

The Gram-Schmidt process [13] provides a easy and recursive way to create an orthogonal or orthonormal base for any linear independent set of vector in $\mathbb{R}^n$

Gram-Schmidt Algorithm

1: **INPUT** $\beta = \{\vec{b}_1, \vec{b}_2, ..., \vec{b}_k\}$ in $\mathbb{R}^n$

2: $\vec{u}_1 = \vec{b}_1$

3: for $p = 2$ to k

4: $\quad \vec{u}_p = \vec{b}_p - \sum_{i=1}^{p-1} \frac{\langle \vec{b}_p, \vec{u}_i \rangle}{\langle \vec{u}_i, \vec{u}_i \rangle} \vec{u}_i$

5: endfor

6: **OUTPUT** $U = \{\vec{u}_1, \vec{u}_2, ..., \vec{u}_k\}$ **in** $\mathbb{R}^n$:= is an orthogonal base.

Now, it is possible to create an *orthonormal* base by applying (Equation 2.7) to each $\vec{u} \in U$.

$$\vec{u}_i' = \frac{1}{\| \vec{u}_i \|} \vec{u}_i \qquad 1 \leq i \leq k \tag{2.7}$$

The following theorem enables to decompose every vector $\vec{x} \in X$ in two parts: the part $\vec{y}$ belonging to the subspace Y of X, and the part $\vec{y}^{\perp}$ that is orthogonal to Y

Theorem 2 ([12]). For any linear subspace Y of X,

$$X = Y \oplus Y^{\perp}. \tag{2.8}$$

Proof. [12] We show first that a decomposition of form (Equation 2.8)' is unique. Suppose we could write

$$\vec{x} = \vec{z} + \vec{z}^{\perp}, \qquad \vec{z} \text{ in } Y,\ z^{\perp} \text{ in } Y^{\perp} \tag{2.9}$$

Compared with (Equation 2.8)' gives

$$\vec{y} - \vec{z} = \vec{z}^{\perp} - \vec{y}^{\perp}, \tag{2.10}$$

it follows from this that $\vec{y} - \vec{z}$ belongs both to Y and to $Y^{\perp}$, and thus is orthogonal to itself:

$$0 = (\vec{y} - \vec{z}, \vec{z}^{\perp} - \vec{y}^{\perp}) = (\vec{y} - \vec{z}, \vec{y} - \vec{z}) = \| \vec{y} - \vec{z} \|, \tag{2.11}$$

but by positivity of norm, $\vec{y} - \vec{z} = 0$ or $\vec{y} = \vec{z}$.

To prove that a decomposition of form (Equation 2.8) is always possible, we construct an orthogonal basis of X whose first k members lie in Y; the remainder must lie in $Y^{\perp}$ We can construct such a basis by starting with an orthogonal basis in Y, afterwards complete it to a basis in X, and then creating an orthogonal base with the remainder vectors of the basis computing the *Gram-Schmidt process.* Afterwards, $\vec{x}$ can be decomposed as follows:

$$\vec{x} = \sum_{j=1}^{n} a_j \vec{x}^{(j)} \tag{2.12}$$

We break this decomposition into two parts:

$$\vec{x} = \sum_{j=1}^{n} a_j \vec{x}^{(j)} = \sum_{j=1}^{k} a_j \vec{x}^{(j)} + \sum_{l=k+1}^{n} a_l \vec{x}^{(l)} = \vec{y} + \vec{y}^{\perp}; \tag{2.13}$$

clearly, $\vec{y}$ lies in Y and $\vec{y}^{\perp}$ in $Y^{\perp}$ $\square$

After this theorem is a good idea to define the concept of *magnitude of a vector.*

Definition 7. The **magnitude of a vector** $\vec{v}$ is denoted by $\| \vec{v} \|$ and can be calculated using the following equation:

$$\| \vec{v} \| = \sqrt{\langle \vec{v}, \vec{v} \rangle} \tag{2.14}$$

Now, we are ready to describe one of the main tools for methods based on LMM, the *simplex.* Mainly because many of them are looking at methods to obtain simplexes of maximal volume.

Definition 8. A **simplex in** $\mathbb{R}^n$ is a polytope in a n-dimensional space with $(n+1)$ vertices.

The following definition remarks this important concept, and provides a objective to reach by giving a performance measure for the algorithms based on the LMM.

Definition 9. Let X be a set of vectors in $\mathbb{R}^n$, let $\wp$ be the power set of X, and let ξ be the collection of every subset $E \in \wp$, of cardinality $\#E = n+1$. The **Simplex of maximal volume in** $\mathbb{R}^n$ **(SMV**^{n}**)** is any $\hat{E} \in \xi$ such that

$$Vol(\hat{E}) \geq Vol(E_i) \quad 1 \leq i \leq \#\xi$$

Due to the convex nature of the hyperspectral imagery and the LMM assumptions, each vertex in the SMV^{k-1} (Definition 8) is an endmember. Then, for a given HI X, there is a set $E = \{\vec{e}_0, \vec{e}_1, ..., \vec{e}_{k-1}\} \subset X$ of endmembers and the reminder $X \setminus E$ spectral pixels are linear combinations of elements of E. Furthermore, $\#E$ is very small respect to N. Therefore, the problem of endmember extraction is equivalent to the problem of finding a set of vertices within the SMV^{k-1}

Winter [8] said that the volume of a simplex is proportional to (Equation 3.4). Equivalently, *Peter Lax* [12] provides the elementary formula to calculate the volume of a simplex in $\mathbb{R}^n$:

$$Vol(E) = \frac{1}{n} Altitude \text{ x } Vol_{n-1}(Base), \tag{2.15}$$

where $n = \#E$, $Base$ is any of the $n-1$ dimensional faces of E, and $Altitude$ means the distance between the vertex opposite to the hyperplane spanned by the $Base$. In short $h_n = Altitud$, and $\beta_n = Base$. In a recursive way, this can be expressed as follows:

$$\begin{aligned} Vol(E) &= \frac{1}{n} Altitude \text{ x } Vol_{n-1}(Base) \\ &= \frac{1}{n} h_n \text{ x } Vol(\beta_n) \\ &= \left(\frac{h_n}{n}\right) Vol(\beta_{n-1}) \\ &= \left(\frac{h_n}{n}\right)\left(\frac{h_{n-1}}{n-1}\right) Vol(\beta_{n-2}) \\ &= \left(\frac{h_n}{n}\right)\left(\frac{h_{n-1}}{n-1}\right) \cdots \left(\frac{h_1}{1}\right) \\ &= \frac{(h_n)(h_{n-1})\ldots(h_1)}{n!} \\ &= \prod_{i=1}^{n} \frac{h_i}{i} \end{aligned} \tag{2.16}$$

Unlike to (Equation 3.4), (Equation 2.16) does not require to guaranty the existence of the determinant of a non-singular matrix.

2.3 Fuzzy Logic

The *fuzzy sets* are the basis for the fuzzy analysis. Before to introduce a definition for this important concept, it is necessary to define the classic sets. This thesis refers to the classic sets as *crisp sets*.

Let $\mathbb{U}$ be the universal set. A set is defined by a function, usually called *characteristic function*, that declares which elements of $\mathbb{U}$ are members of the set and which are not [15].

Definition 10 ([15]). The **crisp set** A is defined by its characteristic function,

$$\mathbb{U}_A : \mathbb{U} \rightarrow \{0, 1\},$$

as follows:

$$\mathbb{U}_A(u) = \begin{cases} 1 & \text{for } u \in A \\ 0 & \text{for } u \notin A \end{cases} \tag{2.17}$$

For each $u \in \mathbb{U}$, when $\mathbb{U}_A(u) = 1$, u is declared to be a member of A; when $\mathbb{U}_A(u) = 0$, u is declared as a nonmember of A [15]. This function can be generalized such that the values assigned to the elements of the $\mathbb{U}$ fall within a specified range (typically [0,1]), and it indicates the membership grade of these elements in the set in question. Larger values denote higher degrees of set membership. Such a function is called a *membership function*, and the set defined by it a *fuzzy set.* In this case, each membership function maps elements of $\mathbb{U}$, which is always a crisp set, into real numbers in $[0, 1]$ [15].

Definition 11 ([15]). The **fuzzy membership function** of a fuzzy set A is denoted by μ_A; that is:

$$\mu_A : \mathbb{U} \rightarrow [0, 1] \tag{2.18}$$

The intersection, union, and product operations between two arbitrary fuzzy sets A and B are defined as follow:

$$A \cap B \ := min\,[A(u), B(u)] \tag{2.19}$$

$$A \cup B \ := max\,[A(u), B(u)] \tag{2.20}$$

$$A \times B \ := prod\,[A(u), B(u)] \tag{2.21}$$

The following definition is used to express similarity between two or more spectral pixels.

Definition 12 ([15]). A **fuzzy relation** is a fuzzy set defined on the Cartesian product of crisp sets $X_i, X_2, ..., X_n$, where tuples $x_1, x_2, ..., x_n$ may have varying degrees of membership within the relation. The membership grade indicates the strength of the relation present between the elements of the tuple.

Let $R(X, X)$ be a *fuzzy relation.* For convenience, R is represented by a fuzzy matrix M_R [15]:

$$M_R := \begin{bmatrix} R(x_1, y_1) & R(x_1, y_2) & ... & R(x_1, y_n) \\ R(x_2, y_1) & R(x_2, y_2) & ... & R(x_2, y_n) \\ ... & ... & ... & ... \\ R(x_m, y_1) & R(x_m, y_2) & ... & R(x_m, y_n) \end{bmatrix} \tag{2.22}$$

A *fuzzy relation* has the following properties:

1. R is **reflexive** iff $R(x, x) = 1 \quad \forall x \in X$
2. R is **symmetric** iff $R(x, y) = R(y, x) \quad \forall x, y \in X$
3. R is **max min transitive** iff:

$$R(x, z) \geq \max_{y \in A}\{min\{R(x, y), R(y, z)\}\} \quad \text{for each pair } (x, z) \in X^2 \tag{2.23}$$

These concepts are used to obtains a crisp partition from a fuzzy relation.

Definition 13 ([15]). Let A be a fuzzy set and let α be any real number such that $\alpha \in [0, 1]$. The **α-cut** ${}^{\alpha}A$ and the **strong α-cut** ${}^{+\alpha}A$ is defined as follows:

1. ${}^{\alpha}A \quad := \{x | A(x) \geq \alpha\}$
2. ${}^{+\alpha}A \quad := \{x | A(x) > \alpha\}$

For example: $X = \{1, 2, 3, 4\}$

$A = \{(0.2/1), (0.8/2), (0.48/3), (0.6/4)\}$

$= \{0.2, 0.4, 0.16, 0.15\}$

${}^{\alpha}A$	${}^{+\alpha}A$
${}^{0.15}A = \{0.2, 0.4, 0.16, 0.15\}$	${}^{+0.15}A = \{0.2, 0.4, 0.16\}$
${}^{0.2}A = \{0.2, 0.4\}$	${}^{+0.2}A = \{0.4\}$
${}^{0.4}A = \{0.4\}$	${}^{+0.4}A = \{\emptyset\}$

The following definition enables to group similar spectral pixels in classes using their similarity degree.

Definition 14 ([15]). Let R be a Fuzzy Relation. R is a **fuzzy equivalence relation** iff R is *reflexive*, *symmetric* and *max min transitive.*

The *transitive closure* method (Section 4.2) requires the following definition in order to build a *fuzzy equivalence relation.*

Definition 15 ([15]). A **t-norm** is a binary operation on the unit interval that satisfies at least the following axioms for all $a, b, c \in [0, 1]$:

1. t-norm$(a, 1) = a$
2. $b \leq d$ implies t-norm$(a, b) \leq (a, d)$
3. t-norm(a, b) = t-norm(b, a)
4. t-norm$(a$,t-norm$(b, d))$ = t-norm(t-norm$(a, b), d)$

It is necessary to introduce the following two operations before defining the operation *composition* ($\circ$) between *fuzzy relations.*

$$\text{dom}\, R(x) = \max_{y \in Y} R(x, y) \tag{2.24}$$

$$\operatorname{ran} R(y) = \max_{x \in X} R(x, y) \tag{2.25}$$

Thus, the following operation allows to obtain the *max min transitive* relation for a given compatibility relation (*reflexive and symmetric*).

Definition 16 ([15]). Let X, Y, Z be three crisp sets. Let $R : X \times Y \to [0, 1]$, $S : Y \times Z \to [0, 1]$ be two fuzzy relations. The **fuzzy relations composition** of R and S denoted as $R \circ S$ is a fuzzy relation $R \circ S : X \times Z \to [0, 1]$ such that:

$$R \circ S(x, z) := \max_{y \in Y} \text{ t-norm}(R(x, y), S(y, z)) \tag{2.26}$$

This definition is used to obtains the fewest number of different possible partitions of X, and enables the non-endmember discrimination.

Definition 17. A **transitive closure** R_T of a *fuzzy realtion* R, is the relation that is *max-min transitive*, contains $R(X, X)$, and have the fewest number of α-cuts.

The *transitive closure* R_T can be obtained using the *transitive closure method* (Section 4.2), this method can be implemented efficiently because the following theorem.

Theorem 3 ([15]). Let R be a fuzzy compatibility relation *(reflexive and symmetric)* on a finite universal set S with $\#S = n$. Then, the max min transitive closure of R is the relation R^{n-1}

Proof. By contradiction: Suppose that R is a fuzzy compatibility relation *(reflexive and symmetric)* on a finite universal set S with $\#S = n$. Then, R^{n-1} is NOT the max min transitive closure R_T of R.

Thus, consider a cycle of length n.

$$s_1 R^1 s_2, s_2 R^2 s_3, ..., s_{n-1} R^{n-1} s_n.$$

Based on (Definition 16), we know that $R^2 = R^1 \circ R^1$ such that

$$s_1 R^2 s_3 = s_1 R^1 \circ R^1 s_3.$$

It is possible to infer the same for R^3

$$R^3 = R^2 \circ R^1 = R^1 \circ R^1 \circ R^1$$

such that

$$s_1 R^3 s_4 = s_1 R^2 \circ R^1 s_4 = s_1 R^1 \circ R^1 \circ R^1 s_4.$$

It is possible to repeat this procedure for R^{n-1}

$$R^{n-1} = R^{n-2} \circ R^{n-3}, ..., \circ R^1,$$

therefore,

$$x_1 R^{n-1} x_n.$$

Based on the hypothesis's antecedent, $R^{n-1} \neq R_T$ then, for a natural number $m > n-1$, there exists a relation R^m, such that $R^m = R_T$. By definition of the *Transitive Closure* R_T, R^m must to be the smallest relation R^m that contains all other relations, then, m is fixed to n, thus, the smallest cycle in $R^{m=n}$ is

$$s_1 R^1 s_2, s_2 R^2 s_3, ..., s_{n-1} R^{n-1} s_n, s_n R^{m=n} s_{n+1}.$$

Clearly,

$$\#S = n + 1 \quad \lightning (contradiction).$$

Due to $\#S = n$ (by hypothesis), this contradicts the antecedent of the hypothesis.

$\therefore$ R^{n-1} is the max min *transitive closure* R_T of R. $\square$

Chapter 3

Literature Review

This chapter introduces the approaches typically used for *endmember extraction* and *virtual dimensionality* estimation in the hyperspectral images analysis. Afterwards, it provides a detailed description of several algorithms based on similar principles as the proposed algorithms.

3.1 Approaches

3.1.1 Linear Mixing Models (LMM)

The spacial resolution refers to the area represented in a HI. Such area depends on the HSI's characteristics and the distance between the HSI and the scene. The total area represented in a HI can spans kilometers, thus, the spanned area of each pixel in the HI is equivalent to square meters. For example, for the AVIRIS project [1], the covered area at each pixel is approximately 20 square meters. Making the resolution a main problem because each pixel represent the aggregation of the reflection of different materials. Therefore, the LMM are correlated with the spacial resolution because they assume that the spectral signatures of different materials are mixed by the instruments itself. The main aim of the endmember extraction algorithms based on the LMM is to identify pure pixels where only one type of material is present and use them to unmix the HI into the respective mixture map of the material's abundances [8]. For many applications, this approach is useful because the convex nature of a HI provides an easy and valid way for

its analysis.

The main LMM's drawback is that for many cases, the reflectance is not a linear function due to the fact that many materials present in the scene are hidden for the HSI and they contribute to the sensed spectral signatures.

Let X be a HI. Assuming that the LMM is a well approximation, there is a small set $E \subset X$ of endmembers or pure pixels, and every element of the remainder set of spectral pixels

$$\bar{E} = X \setminus E$$

is composed by a fraction of each element $\vec{e} \in E$ such that the sum of fractions is the total area represented by that spectral pixel. Thus, for all $\vec{x} \in \bar{E}$:

$$\vec{x}_{li} = \sum_{k=1}^{\#E} (\vec{e}_{lk} \times \vec{\alpha}_{ki}) + \omega, \quad 1 \leq i \leq \#\bar{E}. \tag{3.1}$$

In (Equation 3.1), $\vec{x}_{li}$ is the l-th dimension of the i-th spectral pixel in $\bar{E}$, $\vec{e}_{lk}$ is the l-th dimension of the k-th endmember in E, $\vec{\alpha}_{ki}$ is the k-th endmember fraction of the i-th spectral pixel in $\bar{E}$, and ω is a small Gaussian random error. In addition, the endmember fraction α is restricted by:

$$\text{Nonnegativity} \quad \alpha_{ki} \geq 0 \tag{3.2}$$

$$\text{Sum to one} \quad \sum_{k=1}^{\#E} \alpha_{ki} = 1 \tag{3.3}$$

Therefore, the endmembers in the LMM inscribe the simplex in $\mathbb{R}^{k-1}$ of maximum volume [8].

3.1.2 Nonlinear Mixing Models (NMM)

Unlike LMM, NMM considers all physical interactions between photons and the materials in the scene. Thus, this model requires to know prior information about all materials preset in a scene and their molecular composition. The NMM are not as easy as the LMM despite the Radiative Transfer Theory (RTT) [20] is a mature mathematical model that describes how the photons interact with the materials present in the scene. Therefore, RTT require to have knowledge about the physical composition of the materials sensed in the HI. Making quite difficult to obtain the necessary parameters for the model and one of its main drawbacks. Therefore, only a few algorithms address this problem as a total NMM [21]. Nevertheless, there are some attempts [22, 23] to address this drawback by using machine learning methods as neural networks [22–24] to obtain the physical parameters for the RTT, by assuming the prior knowledge of the endmember spectral signature. Recently, Close et al. [25] proposed to generalize the physic interaction by assuming that all pixels are a combination of LMM and NMM. This has allowed to obtain better performance than the traditional existing techniques based on physical mixing parameters.

3.2 Endmember Extraction Algorithms (EEA)

This type of algorithms assume that there is at least one pure pixel or endmember present in a HI. Making the main aim to identify at least this single pixel. This approach is probably the most often used in hyperspectral unmixing applications. The following algorithms are described in order to provide an overview about the existing literature of this type of algorithms.

3.2.1 Pixel Purity Index (PPI) [10]

The PPI algorithm applies dimensional reduction, by setting the purity index for each pixel to zero. Then, the algorithms projects each pixel onto *skewers* defined using a random process. The purity index increases by one every time that the pixel is extreme

in every *skewer* direction. At the termination, the pixels with the maximum value of purity index are selected as endmembers.

3.2.2 The Vertex Component Analysis (VCA) [26]

The VCA algorithm obtains the subspace of maximum volume inscribed by only one vertex. Afterwards, it increases iteratively the number of endmembers in the projection data subspace and selecting the extreme pixel as the new endmember until all endmembers are extracted.

3.2.3 The Sequential Maximum Angle Convex Cone (SMACC) [27]

The SMACC algorithm uses a bottom-up approach based on the convex cone. At the begging, SMACC selects any pixel as endmember (typically that with the maximal length), and it uses this to define a cone. Afterwards, it creates a new cone by adding the pixel with the maximal angle respect to the existing cone until all pixels are inside the cone in a tolerance threshold.

3.2.4 The Simplex Growing Algorithm (SGA) [9]

The SGA algorithm uses a bottom-up approach and requires the number of endmembers to extract as an initial input parameter. Iteratively adds to the list of endmembers the spectral pixel that generates the simplex of maximal volume in a superior dimension by applying the (Equation 3.4).

3.2.5 N-FINDR Algorithm

In 1999 Michael E. Winter published the N-FINDR [8] algorithm, it has been subject of extensive studies and different implementations through the literature. The main idea of the N-FINDR is to find the vertices that maximize the volume of a simplex covering all the pixels in the HI. It receives two parameters: a HI X, and the number $k \in \mathbb{N}$ of endmembers to extract. In addition, N-FINDR requires a HI with dimensionality equal to $k-1$. If the X's dimensionality is bigger than $k-1$, this algorithm applies a dimensionality reduction method as MNF [28], NAPC [29] or PCA [30]. Afterwards,

searches for the set E of k spectral pixels $\vec{x} \in X$ that inscribes the simplex in $\mathbb{R}^{(k-1)}$ of maximum volume in X using (Equation 3.4).

$$Vol(E) = \frac{1}{(k-1)!}|det(E)| \tag{3.4}$$

Thus, N-FINDR initializes the set $E = \{\vec{x}_1, \vec{x}_2, ..., \vec{x}_k\}$, taking k different pixels from X, selects each of them randomly. Then, it calculates the volume of E using (Equation 3.4) in the following way: it swaps in and out each element in E with all pixels in the remainder set $X \setminus E$, calculates the new volume using (Equation 3.4) and replaces the element in E with the pixel in $X \setminus E$ when the new volume is bigger. This procedure is repeated until no one substitution increases the volume. This algorithm is computationally complex because it performs the calculation of (Equation 3.4) several times. Moreover, the algorithm can be considered non-deterministic as its results depend on a random initialization process.

FINDR Algorithm

1: **INPUT** $\mathbf{X} \equiv [\vec{x_1}, \vec{x_2}, ..., \vec{x_N}]$

2: **INPUT** $K \equiv$ Number of endmembers to extract.

3: R = MNF(X, L , k) $\equiv$ NAPC(X, L . k)

4: E = $\{\emptyset\}$

5: for 1 to k

6: $r = rand(N);$ $\quad \vec{e_r} \notin E$

7: $E = E \cup \left\{ \begin{bmatrix} 1 \\ \vec{e_r} \end{bmatrix} \right\};$ $\quad \vec{e_r} \in R$

8: endfor

9: auxVol = 0

10: while(Vol(E) > auxVol)

11: auxVol = Vol(E)

12: tmpVol = Vol(E)

13: for i=1 to N

14: for p=1 to k

15: $\vec{e_r} = \begin{bmatrix} 1 \\ \vec{e_i} \end{bmatrix}$ $\quad \vec{e_r} \notin E, \quad \vec{e_i} \in R$

16: $\Delta = E \oplus \{\vec{e_p} \cup \vec{e_r}\}$ $\quad \vec{e_p} \in E$

17: if(Vol(Δ) > tmpVol)

18: tmpVol = Vol(Δ)

19: $E = \Delta$

20: endif

21: endfor

23: endfor

24: endwhile

25: **OUTPUT** $E = \{\vec{e_1}, \vec{e_1}, ..., \vec{e_K}\}$ $E \equiv$ List of endmebers extracted.

3.2.6 Automatic Target Generation Process (ATGP)

The ATGP is an algorithm proposed by Chein I. Chang [16] to generates a matrix of k pure spectral signatures of a HI X based on the Orthogonal Subspace Projection (OSP) approach. In addition, this algorithm requires to know the number of endmembers present in a HI. It process is as follows: At the beginning, ATGP selects the pixel $\vec{x} \in X$ denoted as $\vec{e}_0$ of maximum length, and uses it to creates an orthogonal subspace structure:

$$P_E^{\perp} = I - E(E^T E)^{-1} E^T \tag{3.5}$$

where $E = \{\vec{e}_0\}$ and I is the identity matrix. Once $P_E^{\perp}$ is computed, ATGP obtains the pixel $\vec{x} \in X \setminus E$ with the maximum orthogonal subspace projection $\langle \vec{e}_0 \rangle^{\perp}$ denoted as $\vec{e}_1$, considering it as the distance of $\vec{e}_1$ respect to the subspace spanned by the structure $P_E^{\perp}$. Afterwards, $\vec{e}_1$ is added to E such that $E = \{\vec{e}_0, \vec{e}_1\}$. Then, for $1 \leq i < k$ iteration, ATGP considers that $\vec{e}_i$ is the pixel $\vec{x} \in X \setminus E$ with the maximum orthogonal subspace projection $\langle \vec{e}_0, \vec{e}_1, ..., \vec{e}_{i-1} \rangle^{\perp}$ using (Equation 3.5). Then, it adds $\vec{e}_i$ to E such that $E = \{\vec{e}_0, \vec{e}_1, ..., \vec{e}_i\}$ until $\#E = k$, relying that each pixel $\vec{e} \in E$ is an endmember.

Automated Target Generation Process (ATGP)

1: **INPUT** $\mathbf{X} \equiv [\vec{x_1}, \vec{x_2}, ..., \vec{x_N}]$

2: **INPUT** $K \equiv$ Number of endmembers to extract.

3: $E = \{ \arg\max_{\vec{x_i}} (\|\vec{x_i}\|) \}$ $\quad 1 \leq i \leq N,\ i \in \mathbb{N}$

5: for $k = 1$ to $(K - 1)$

6: $\quad P_{E^{\perp}} = I - E(E^T E)^{-1} E^T$

7: $\quad E \cup \{ \arg\max_{\vec{x_i}} ([P_{E^{\perp}} \vec{x_i}]\,[P_{E^{\perp}} \vec{x_i}]) \}$ $\quad 1 \leq i \leq N,\ i \in \mathbb{N}, \vec{x_i} \notin E$

8: endfor

9: **OUTPUT** $E = \{\vec{e_0}, \vec{e_1}, ..., \vec{e_{K-1}}\} \equiv$ List of endmembers extracted.

3.2.7 Orthogonal Bases Approach (OBA)

OBA is an algorithm introduced by Xuetao Tao et al. [11] at 2009. Its main aim is to find the orthogonal base of maximal norm using the Gram-Schmidt orthogonalization process by assuming that the Gram determinant is equivalent to the volume equation (Equation 3.4) used by N-FINDR. The OBA's process is as follows: for a given HI X, it requires the number $k \in \mathbb{N}$ of endmembers to extract. If k is unknown, it works in an automatic way by setting the threshold parameter ω (the author recommends to set $\omega = 3.3$). Thus, it extracts the spectral pixel $\vec{x} \in X$ of maximal length and defines this as the endmember $\vec{e}_0$. Subsequently, it selects the spectral pixel $x \in X$ which has the maximal magnitude after being subtracted from $\vec{e}_0$ as follows:

$$\vec{e}_1 = arg\ max_{\vec{x}_i} (\parallel \vec{x}_i - \vec{e}_0 \parallel) \qquad 1 \leq i \leq \#X$$

Then, it extracts the remainder $k - 1$ endmembers or extracts the endmembers one by one, using the iterative Gram-Schmidt orthogonalization process until the norm of the orthogonal base decrease to a lower value than the specified threshold ω.

It is very important to remark that, OBA does not creates an orthogonal base with the original vectors because it works with the set of vectors $\vec{l_i}$ for $1 \leq i \leq \#X$ (7-th line). $\vec{l_i}$ is obtained by subtracting to the vector chosen as origin $\vec{e}_0$, every spectral pixel $\vec{x} \in X$ as follows:

$$\vec{l_i} = \vec{x}_i - \vec{e}_0 \qquad 1 \leq i \leq \#X.$$

Due to the endmembers extraction algorithm proposed in this thesis uses the original spectral pixels in X, and it considers the orthogonal complement instead of the vector subtraction, it was possible to improve the performance obtained by OBA. A detailed description is introduced in (Section 4.1).

Orthogonal Bases Approach (OBA)

1: **INPUT X** $\equiv [\vec{x_1}, \vec{x_2}, ..., \vec{x_N}]$

2: **INPUT** $K \equiv$ Number of endmembers to extract.

3: //Initialization

4: $e_0 = arg\ max_{x_i} (\parallel x_i \parallel)$

5: $e_1 = arg\ max_{x_i} (\parallel x_i - e_0 \parallel)$

6: $\alpha_1 = e_1 - e_0$, $\beta_1 = \alpha_1$

7: $l_i = x_i - e_0$, (i=1,...,N)

8: $\gamma_i^1 = l_i - \left(\frac{\langle l_i, \beta_1 \rangle}{\langle \beta_1, \beta_1 \rangle}\right) \beta_1$, ($i$=1,...,N)

9: $k = 1$

10: //Main loop

11: **while** stopping condition is not met **do**

12: $e_{k+1} = arg\ max_{x_i} (\parallel \gamma_i^k (x_i) \parallel)$

13: $\beta_{k+1} = arg\ max_{x_i} (\parallel \gamma_i^k \parallel)$

14: $\gamma_i^{k+1} = \gamma_i^k - \left(\frac{\langle l_i, \beta_{k+1} \rangle}{\langle \beta_{k+1}, \beta_{k+1} \rangle}\right) \beta_{k+1}$ (i=1,...,N)

15: Increase k by 1

16: **end**

17: **OUTPUT** $E = \{\vec{e_0}, \vec{e_1}, ..., e_{\vec{K-1}}\} \equiv$ List of endmebers stimated.

3.3 Virtual Dimensionality Estimation Algorithms

This section introduces a description of the algorithms often used in the literature to estimate the Virtual Dimensionality (VD) (Definition 5). This concept was introduced by Chang [14] at 2003 to estimate the number of distinct signals present in a hyperspectral data. Due to the fact that each signal in the VD is an endmember, it is used to set the number $k \in \mathbb{N}$ of endmembers present in a HI that is required by several EEAs as an input parameter.

3.3.1 Harsanyi-Ferrand-Chang (HFC)

The HFC [5] algorithm calculates the eigenvalues for the sample correlation Matrix $\mathbf{R}$ and the sample covariance matrix $\mathbf{M}$. Let $\{\hat{\lambda}_1, \hat{\lambda}_2, ..., \hat{\lambda}_L\}$ and $\{\lambda_1, \lambda_2, ..., \lambda_L\}$ be the set of eigenvalues of $\mathbf{R}$ and $\mathbf{M}$ respectively (L is the number of dimensions). The HFC algorithm assumes that the spectral signal sources are non-random unknown positive constants with zero mean noise and using hypothesis testing infers:

$$\hat{\lambda}_i > \lambda_i \qquad \text{for } i = 1, 2, ..., VD \tag{3.6}$$

and

$$\hat{\lambda}_i = \lambda_i \qquad \text{for } i = (VD+1), (VD+2), ..., L \tag{3.7}$$

relating (Equation 3.6) and (Equation 3.7) by

$$\hat{\lambda}_l > \lambda_l > \sigma^2_{n_l} \qquad \text{for } l = 1, 2, ..., VD \tag{3.8}$$

and

$$\hat{\lambda}_l = \lambda_l = \sigma^2_{n_l} \qquad \text{for } l = VD+1, VD+2, ..., L. \tag{3.9}$$

Thus, the HFC formulates the VD estimation as the binary hypothesis

$$H_0 : z_l = \hat{\lambda}_l - \lambda_l = 0 \qquad \text{for } l = 1, 2, ..., L \tag{3.10}$$

versus

$$H_1 : z_l = \hat{\lambda}_l - \lambda_l > 0 \qquad \text{for } l = 1, 2, ..., L. \tag{3.11}$$

Assuming that N is sufficient large to model H_0 and H_1 as random variables by the conditional probability densities:

$$p_0(z_l) = p(z_l|H_0) \cong N(0, \sigma_{z_l}^2) \qquad \text{for } l = 1, 2, ..., L \tag{3.12}$$

and

$$p_1(z_l) = p(z_l|H_1) \cong N(\mu_l, \sigma_{z_l}^2) \qquad \text{for } l = 1, 2, ..., L. \tag{3.13}$$

$\sigma_{z_l}^2$ for each $l = 1, 2, ..., L$ using (Equation 3.14)

$$\begin{aligned} \sigma_{z_l}^2 &= var\left[\hat{\lambda}_l - \lambda_l\right] \\ &= var\left[\hat{\lambda}_l\right] + var\left[\lambda_l\right] - 2\text{cov}(\hat{\lambda}_l, \lambda_l) \end{aligned} \tag{3.14}$$

where

$$var\left[\hat{\lambda}_l\right] \cong \frac{2\hat{\lambda}_l^2}{N} \tag{3.15}$$

and

$$var\left[\lambda_l\right] \cong \frac{2\lambda_l^2}{N}. \tag{3.16}$$

(Equation 3.10) and (Equation 3.11) formulate a Neyman-Pearson detector $\delta_{NP}(\hat{\lambda}_l - \lambda_l)$ used to maximize the probability detection power

$$P_D = \int_{\alpha}^{\infty} p_1(z)dz \tag{3.17}$$

and minimize the false alarm probability

$$P_F = \int_{\alpha}^{\infty} p_0(z)dz \tag{3.18}$$

at a specific threshold parameter α. Therefore, if $\hat{\lambda}_l - \lambda_l > \alpha$, HFC assumes the existence of a signal energy contributing to the eigenvalue $\hat{\lambda}_l$, in the l-th data dimension. HFC interprets the total number of dimensions with energy present as the number of endmembers present in the HI.

3.3.2 Noise-Whitened-Harsanyi-Ferrand-Chang (NWHFC)

Due to the fact that HFC assumes that the dataset has white Gaussian noise with zero mean and the spectral signal variance $\sigma^2_{z_l}$ is typically small, its VD estimation can be biased by inter-bands covariance. In order to mitigate that effect, NWHFC performs a preprocessing phase where the variance matrix and covariance matrix are noise whitened. The preprocessing phase can be done by applying the method proposed by Roger et al. in [36]. Afterwards, the HFC method is performed to the new covariance and correlation matrix.

3.3.3 Eigenvalue Distribution-Based Criteria (EDBC)

It is a set of methods to estimate the number of different signals present in a dataset based on the sum of correlation and covariance eigenvalues. In order to do this, this type of methods require to set a parameter α, *stop condition*. Furthermore, the correlation eigenvalues $\hat{\lambda}_1, \hat{\lambda}_2, ..., \hat{\lambda}_L$ and the covariance eigenvalues $\lambda_1, \lambda_2, ..., \lambda_L$ must to be normalized using (Equation 3.19) and (Equation 3.20).

$$\hat{\lambda}_l = \frac{\hat{\lambda}_l}{\sum_{l=1}^{L} \hat{\lambda}_l} \tag{3.19}$$

$$\lambda_l = \frac{\lambda_l}{\sum_{l=1}^{L} \lambda_l} \tag{3.20}$$

where $\hat{\lambda}_1 \geq \hat{\lambda}_2 \geq, ..., \geq \hat{\lambda}_L$ and $\lambda_1 \geq, \lambda_2 \geq, ..., \geq \lambda_L$. Once the eigenvalues are normalized, it is possible to apply the following methods.

3.3.3.0.1 Test Modified Paragraph

The Threshold Energy Percentage (TEP) method [16] considers that the normalized eigenvalue represents how much percentage energy is contributed by the signal source. Therefore, TEP counts for the number of eigenvalues while the cumulative energy is lower than $\alpha\%$, by using:

$$VD_{\hat{\lambda}_l}^{eigen}(\alpha\%) = arg\left\{ min_{1\leq l\leq L}\left[\sum_{l=1}^{L}\hat{\lambda}_l \geq \frac{\alpha}{100}\right]\right\} \qquad \alpha \in (0,100] \tag{3.21}$$

3.3.3.0.2 Thresholding Difference Between Normalized Correlation Eigenvalues and Normalized Covariance Eigenvalues

Analogous to HFC, it is based on the assumption that $\hat{\lambda}_l - \lambda_l > 0$ when a signal energy is contributing in the dimension l. Therefore, it is possible to estimate VD as follows:

$$VD_{\hat{\lambda}_l-\lambda_l}^{eigen}(\alpha) = arg\{max_{1\leq l\leq L}\left[\hat{\lambda}_l - \lambda_l \geq \alpha\right]\} \qquad \alpha \in [0,1] \tag{3.22}$$

3.3.3.0.3 Finding First Sudden Drop in the Normalized Eigenvalue Distribution

This method calculates the distance between each adjacent pair of correlation or covariance eigenvalues $\delta_1, \delta_2, ..., \delta_{L-1}$ such that $\delta_l = \hat{\lambda}_l - \hat{\lambda}_{l+1}$ or $\delta_l = \lambda_l - \lambda_{l+1}$, and $1 \leq l < L$. Afterwards, it counts the number of values δ_l that are bigger or equal than α as follows:

$$VD_{\hat{\lambda}}^{eigen}(\alpha) = arg\{max_{1\leq l<L}\left[\hat{\lambda}_l - \hat{\lambda}_{l+1} \geq \alpha\right]\} \qquad \alpha \in [0,1], \tag{3.23}$$

or

$$VD_{\lambda}^{eigen}(\alpha) = arg\{max_{1\leq l<L}\left[\lambda_l - \lambda_{l+1} \geq \alpha\right]\} \qquad \alpha \in [0,1]. \tag{3.24}$$

This page is intentionally left blank.

Chapter 4

Proposed algorithms

This chapter introduces a detailed description of the algorithms proposed for endmembers extraction in a HI, it describes their differences and advantages respect to the algorithms presented in the literature review.

4.1 Simplex of Maximal Volume using Perpendicular Altitude (SMV⊥)

The SMV⊥ algorithm is an EEA developed for fast endmembers extraction. This algorithm improves some of the main drawbacks of the often used algorithms of the literature review of the EEAs for hyperspectral image analysis. Then, the description of the SMV⊥'s procedure is introduced.

Let X be a HI (Definition 1) with N *spectral pixels* (Definition 2) and L dimensions. Suppose that it is required to extract $k \in \mathbb{N}$ endmembers from X. Let $\xi = \{E_1, E_2, ..., E_n\}$ be the set of all subsets $E_i \subset X$ of cardinality equal to k, where $1 \leq i \leq n$.

Based on the LMM, there exists a set $\hat{E} \in \xi$ that is the SMV^{k-1} such that

$$vol(\hat{E}) \geq vol(E_i),$$

for all $E_i \in \xi$. Due to $\hat{E}$ is the SMV^{k-1} (Definition 9), every $\vec{e} \in \hat{E}$ is an endmember of X. Therefore, the remainder pixels in $X \setminus \hat{E}$ are linear combination of $\hat{E}$. Thus, the extraction of endmembers is described as follow.

1) Extracting $\vec{e}_1$: At the beginning, SMV⊥ sets the set of endmembers $E = \{\emptyset\}$. The (Equation 2.16) shows that the volume of the set $\hat{E}^1$ ($\#E^1 = 1$), is the distance of the unique member $\vec{e}_1 \in \hat{E}^1$ respect to the subspace spanned by the set $\hat{E}^1 \setminus \vec{e}_1 = \{\emptyset\} =$ *null space*. Due to every vector is orthogonal to the *null space* then, the orthogonal complement $\vec{e}_1^{\perp}$ (Definition 6) is $\vec{e}_1$ itself. Therefore, the altitude $\vec{h}_1$ of $\vec{e}_1$ respect to the *null space* is the magnitude of $\vec{e}_1$ using (Equation 2.14) such that:

$$h_1 = vol(\hat{E}^1) = \| \vec{e}_1 \| = \sqrt{\langle \vec{e}_1, \vec{e}_1 \rangle} \tag{4.1}$$

Then, SMV⊥ considers that the *spectral pixel* $\vec{x} \in X$ with the maximal magnitude using (Equation 2.14) is the endmember $\vec{e}_1$ because it is the SMV^0 (Definition 9). The SMV⊥ extracts $\vec{e}_1$ at the fourth line, adds $\vec{e}_1$ to the set of extracted endmembers E, and define the orthogonal base $U = \{\vec{e}_1\}$.

2) Extracting $\vec{e}_j$ $(2 \leq j \leq K)$: A very important observation derived from (Equation 2.16) is: the height $\vec{h}$ of any $\vec{e} \in \hat{E}$ respect to the subspaces spanned by the set of vectors $\hat{E} \setminus \vec{e}$ is bigger or equal than every height $\vec{h}_x$ of all *spectral pixels* $\vec{x} \in X$ respect to the subspace spanned by $\hat{E} \setminus \vec{e}$. Moreover, if any vertex of $\hat{E}$ is removed, the remainder set $\hat{E}' = \hat{E} \setminus \vec{e}$ maintains this property. The SMV⊥ considers for every *spectral pixel* $\vec{x} \in X$ that its distance h_x is equal to the magnitude of the orthogonal complement $\vec{x}^{\perp}$ respect to the orthogonal base discovered U. In order to obtain $\vec{x}^{\perp}$, SMV⊥ exploits the capability of *Gram-Schmith Algorithm* to calculate the orthogonal projection $\vec{x} \mapsto U$ of any $\vec{x}$ over the subspace spanned by the orthogonal base U (*Gram-Shmith Algorithm at line 4*) and defines the following equation:

$$\vec{x} \mapsto U = \sum_{i=1}^{m} \frac{\langle \vec{x}, \vec{u}_i \rangle}{\langle \vec{u}_i, \vec{u}_i \rangle} \vec{u}_i \qquad m = \#U,\ \vec{u}_i \in U \tag{4.2}$$

Once calculated the orthogonal projection $\vec{x} \mapsto U$, SMV⊥ uses the (Theorem 2) to define the following equation in order to calculate the orthogonal complement $\vec{x}^{\perp}$:

$$\vec{x}^{\perp} = \vec{x} - (\vec{x} \mapsto U) \tag{4.3}$$

At iteration j, SMV⊥ considers that the *spectral pixel* $\vec{x} \in X$ with the $\vec{x}^{\perp}$ (Equation 4.3) of maximal magnitude using (Equation 2.14) is the endmember $\vec{e}_j$. Then, it adds $\vec{e}_j$ to the set E of extracted endmembers, and creates the new orthogonal base $U = U \cup \{\vec{x}^{\perp}\}$. This is repeated $K - 1$ times.

Thus, due to the SMV⊥ obtains at each iteration i, the pixel $\vec{x} \in X$ with the maximal height h_i respect to the subspace spanned by the base U formed with the set E of vectors extracted as endmembers at iteration $i - 1$, by starting in the *null space*, and the volume equation (Equation 2.16) multiplies the volume of the base U by h_i in order to calculates the volume of the simplex in $\mathbb{R}^{\#U}$. SMV⊥ guarantees that the simplex in $\mathbb{R}^{\#U}$ is which has the maximal volume then, it is the Simplex of Maximal Volume in $\mathbb{R}^{\#U}$ ($SMV^{\#U}$). This SMV⊥'s property is very important for the EEAs based on LMM because the SMV^n has the property of convexity and it is used to unmix the HI in the respective abundance composition of the endmembers extracted. Furthermore, due to the SMV^n has the maximal volume, the vertices in the set E are the $\#E$ most distinct pixels in the HI. This SMV⊥'s property allows to rely that every pixel $\vec{e} \in E$ represents a different material in the scene. Thus, it enables to create material maps, material detection, and target identification.

4.1.1 Pseudo-Code

The following pseudo-code aims to provide almost a SMV⊥'s implementation. This algorithm requires to estimate the number of endmembers present in X, it is possible to calculate the parameter K using HFC-NWHFC [5] or any other that the user wants.

SMV⊥ Algorithm

INPUT $\mathbf{X} \equiv [\vec{x}_1, \vec{x}_2, ..., \vec{x}_N] \equiv$ A hyperspectral image.
INPUT $K \equiv$ Number of endmembers to extract.
j = arg $\max_i (\|\vec{x}_i\|)$ $\quad i = 1, ..., N$
$\mathbb{J} = \{ \text{j} \}$ //Close j
$\vec{u}_1 = \vec{x}_j$
$U = \{\vec{u}_1\}$
$E = \{\vec{x}_j\}$
$\vec{\beta}_i = \vec{0}$ $\quad i = 1, ..., N$
for $k = 2$ to K
  $h_{max} = 0$
  for $i = 1$ to N
    if $(i \notin \mathbb{J})$
      $\vec{\beta}_i = \vec{\beta}_i + \left(\frac{\langle \vec{x}_i, \vec{u}_{k-1} \rangle}{\langle \vec{u}_{k-1}, \vec{u}_{k-1} \rangle} \vec{u}_{k-1} \right)$
      $h_{aux} = \|\vec{x}_i - \vec{\beta}_i\|$
      if ($h_{aux} > h_{max}$)
        $h_{max} = h_{aux}$
        j = i
      endif
    endif
  endfor
  $\mathbb{J} = \mathbb{J} \cup \{ \text{j} \}$
  $\vec{u}_k = \vec{x}_j - \vec{\beta}_j$
  $U = U \cup \{\vec{u}_k\}$
  $E = E \cup \{\vec{x}_j\}$
endfor
OUTPUT $E = \{\vec{e}_1, \vec{e}_2, ..., \vec{e}_K\} =$ {Set of extracted endmembers}.
OUTPUT $U = \{\vec{u}^1, \vec{u}^2, ..., \vec{u}^K\} =$ An orthogonal base for E.

4.2 Fuzzy Virtual Dimensionality (FuzzyVD)

Let X be a hyperspectral image (Definition 1) then, from the (Equation 3.1) it is possible to know that any base $\beta \subset X$ can be used to describe each $\vec{x} \in X$ in terms of β. Now, using (Theorem 1), it is possible to infer that $\#\beta$ is at most L. Therefore, it is possible say that β can be any subset of X. Then, this can be used to decompose each $\vec{x} \in X$ in the abundances of each $\vec{b} \in \beta$. Although this is true, FuzzyVD needs the base β with the maximal volume due to the fact that the vertices on the base β that inscribing the simplex in $\mathbf{R}^n$ of maximal volume, are considered pure pixels (*endmembers*) [8].

Thus, the proposed algorithm FuzzyVD, uses the SMV$\perp$ algorithm to obtains the possible endmembers for a given set of vectors X in $\mathbf{R}^n$, and a number $k \in \mathbb{N} < \#X$, SMV$\perp$ finds a subset $\beta^{\text{SMV}\perp} \subset X$ inscribing the simplex in $\mathbf{R}^k$ of maximal volume using a bottom-up strategy with small computational complexity. Taking advantage from this capability, it is possible to set $k = L$ and calculate the best base $\beta^{SMV\perp}$ composed with all candidates to be endmember using the SMV$\perp$ algorithm.

The next phase of FuzzyVD is to decide if it is feasible to join two or more members of $\beta^{SMV\perp}$, by creating *equivalence classes.* However, to decide if two candidates are similar or not tend to be difficult task. Nevertheless, fuzzy logic provides a natural way to deal with this problem.

In the proposed algorithm, FuzzyVD makes use of *Clustering Method Based Upon Equivalence Relations (CMER)* which was proposed by Klir in [15]. Basically, FuzzyVD uses CMER to calculates the set of α-cuts that induces the different possible partitions with similarity degree α. The first phase of FuzzyVD is to build a square matrix M_R equal to (Equation 2.22) with $\#\beta^{\text{SMV}\perp} = L$ rows and columns. The intersection value in a certain row i and column j represents the relation between the vectors $\vec{b}_i, \vec{b}_j \in \beta^{\text{SMV}\perp}$

calculated the following way:

$$M_R[r_{ij}] := R(\vec{b}_i, \vec{b}_j) \tag{4.4}$$
$$:= 1 - \delta \left(\sum_{l=1}^{L} |b_{il} - b_{jl}|^q \right)^{\frac{1}{q}}$$

where $q \in \mathbb{R}^+$ and represents the type of distance used e.g. $q = 1$ and $q = 2$ are *Hamming distance* and *Euclidean distance* respectively. δ is calculated by (Equation 4.5) in order to ensures that $M_R[r_{ij}] \in [0, 1]$.

$$\delta := \frac{1}{max\left(\left(\sum_{l=1}^{L} |\vec{x}_{il} - \vec{x}_{jl}|^q \right)^{\frac{1}{q}} \right)} \qquad 1 \leq i, j \leq L \tag{4.5}$$

It is possible to see in (Equation 2.22) that M_R is a fuzzy relation between each pair of vectors $\vec{b}_i, \vec{b}_j \in \beta^{\text{SMV}\perp}$ where FuzzyVD use the Euclidean distance $q = 2$. If $\vec{b}_i$ is close to $\vec{b}_j$ then, the $M_R[r_{ij}]$ tend to 1. If the vectors $\vec{b}_i, \vec{b}_j \in \beta^{\text{SMV}\perp}$ are such that the distance between them is bigger or equal than all other pair of vectors in $\beta^{\text{SMV}\perp}$ then, $M_R[r_{ij}] = 0$. Now, if $i = j$, $M_R[r_{ij}] = 1$ (*Reflexive property*). Due to the distance from $\vec{b}_i$ to $\vec{b}_j$ is the same than the distance from $\vec{b}_j$ to $\vec{b}_i$, $M_R[r_{ij}] = M_R[r_{ji}]$ (*Symmetry property*). The remaining pairs have a fuzzy value based in a fuzzy distance calculated using the Minkowski formula defined in (Equation 4.4). Afterwards, CMER creates the transitive closure R_T (Algorithm R_T) using the algorithm provided by Klir in [15] based upon (Definition 16), (Equation 2.19), (Equation 2.20), (Equation 2.21), and (Theorem 3).

Algorithm R_T

1: **INPUT:** $R := M_R :=$ Fuzzy Relation
2: **INPUT:** $n :=$ Universe of discourse cardinality
3: $k = 0$
4: While $2^k < n$
5: $R' = R \cup (R \circ R)$
6: If $R' \neq R$
7: $R = R'$
8: $k = k + 1$
9: Else $R' \neq R$
10: go to Step 13
11: End If
12: End While
13: $R_T = R'$
14: **OUTPUT:** $R_T :=$ Transitive closure

Once applied, the *transitive closure* R_T induces the set $\Delta = \{\alpha\text{-cut}_1, \alpha\text{-cut}_2, ..., \alpha\text{-cut}_m\}$ such that each $\alpha\text{-cut}_i \in \Delta$ represents a crisp equivalence relation of $\beta^{SMV\perp}$ with similarity degree greater or equal than $\alpha\text{-cut}_i$ in R_T. The set Δ can be computed using the following procedure (Algorithm Δ), setting $n = L = \#\beta^{SMV\perp}$

Algorithm Δ

1: **INPUT:** R_T := Fuzzy Transitive Closure
2: **INPUT:** n := Universe of discurse cardinality
3: $\Delta = \{\emptyset\}$
4: For i=1 to n
5: For j=1 to n
6: If $R_T[i,j] \notin \Delta$
7: $\Delta = \Delta \cup R_T[i,j]$
8: End If
9: End For
10: End For
11: **OUTPUT:** $\Delta := \{\alpha\text{-cut}_1, \alpha\text{-cut}_2, ..., \alpha\text{-cut}_m\}$

Then, once R_T has been calculated, the followings set is computed:

$$\Gamma := \{\text{All possible classes induces by } \Delta \text{ in } R_T.\} \tag{4.6}$$

using the procedure (Algorithm Γ) setting $n = L = \#\beta^{SMV^{\perp}}$

Algorithm Γ

1: **INPUT:** R_T := Fuzzy Transitive Closure
2: **INPUT:** Δ := $\{\alpha\text{-cut}_1, \alpha\text{-cut}_2, ..., \alpha\text{-cut}_m\}$
3: **INPUT:** n := Universe of discurse cardinality
4: $\Gamma = \{\emptyset\}$
5: For r=1 to ($\#\Delta$)
6: $OPEN = \{1, 2, ..., n\}$
7: $\Gamma_r = \{\emptyset\}$
8: $i = 1$
9: While $OPEN \neq \{\emptyset\}$
10: $\Gamma_{r,i} = \{\emptyset\}$
11: $Q = \{OPEN(1)\}$
12: $OPEN = OPEN \setminus OPEN(1)$
13: While $Q \neq \{\emptyset\}$
14: $k = Q(1)$
15: $\Gamma_{r,i} = \Gamma_{r,i} \cup Q(1)$
16: $Q = Q \setminus Q(1)$
17: For l=1 to n
18: If $R_T[k, l] \geq \Delta(r)$ and $l \in OPEN$
19: $Q = Q \cup \{l\}$
20: $OPEN = OPEN \setminus \{l\}$
21: End If
22: End For
23: End While
24: $i = i + 1$
25: $\Gamma_r = \Gamma_r \cup \Gamma_{r,i}$
26: End While
27: $\Gamma = \Gamma \cup \Gamma_r$
28: End For
29: **OUTPUT:** $\Gamma := \{\Gamma_1, \Gamma_2, ..., \Gamma_m\}$ = {All possible classes induces by Δ in R_T}.

There exists the correspondence one to one between Δ and Γ, such that for each α-cut$_i \in \Delta$, there is a subset $\Gamma_i \subseteq \Gamma$. In addition, $\#\Gamma_i$ represents the number of disjoint sets in the *fuzzy equivalence relation* induced by an α-cut$_i$ over R_T. Now, Γ generates the minimum finite number of ways on which $\beta^{SMV\perp}$ can be split. Thus, FuzzyVD converts a problem where non prior information exists into another where it is only necessary to find the best α-cut. In order to solve this new problem, FuzzyVD uses a *fuzzy system* to select the α-cut$_i$ that generates the partition with more dense classes, bigger distance between classes' centers, and bigger accumulated energy. The density of each class in the partition $\Gamma_i \in \Gamma$ induced by the α-cut$_i \in \Delta$ is calculated with the following fuzzy membership function:

$$\mu_1(\Gamma_i) := 1 - \left(\frac{1}{\#\Gamma_i} \times \sum_{j=1}^{\#\Gamma_i} \frac{\sigma^2(\Gamma_{i,j})}{\phi_i} \right) \qquad (4.7)$$
$$1 \leq i \leq \#\Gamma$$

where σ^2 is the standard deviation function and Φ_i is:

$$\phi_i := \max(\sigma^2(\Gamma_{i,j})) \qquad (4.8)$$
$$1 \leq i, j \leq \#\Gamma$$

The set $\psi = \{\psi_1, \psi_2, ..., \psi_m\}$ that contains the center in $\mathbb{R}^n$ for all classes in Γ is calculated by using (Algorithm ψ).

Algorithm ψ

INPUT: $\Gamma :=$ Set of all possible classes.
INPUT: $L :=$ Number of dimensions of all $\vec{x} \in X$.
  $\psi = \{\emptyset\}$
  For $i = 1$ to $\#\Gamma$
    $\psi_i = \{\emptyset\}$
    For $j = 1$ to $\#\Gamma_i$
      $\psi_{i,j} = \mathbb{R}^L$
      For $l = 1$ to L
        $\psi_{i,j}(l) = \frac{1}{\#\Gamma_{i,j}} \sum_{k=1}^{\#\Gamma_{i,j}} \Gamma_{i,j,k}(l)$
      End For
      $\psi_i = \psi_i \cup \psi_{i,j}$
    End For
    $\psi = \psi \cup \psi_i$
  End For
OUTPUT: $\psi = \{\psi_1, \psi_2, ..., \psi_m\} = \{$ All classes centers in $\mathbb{R}^n$ $\}$.

Once the set ψ is computed, the distance between the centers of the classes for a given α-cut$_i$ is evaluated using the following fuzzy membership function:

$$\mu_2(\psi, i) := \frac{\sigma^2(\psi_i)}{\Psi}, \quad 1 \leq i \leq \#\Gamma \tag{4.9}$$

where σ^2 is the standard deviation function and Ψ is defined in (Equation 4.10).

$$\Psi := \max(\sigma^2(\psi_i)) \quad 1 \leq i \leq \#\psi \tag{4.10}$$

The energy of an arbitrary

$$\vec{b} \in \beta^{\mathrm{SMV}\perp}$$

is at most the ratio between $\frac{\|\vec{b}_i\|}{\|\vec{b}_0\|}$. This ratio is interpreted by FuzzyVD as the maximum amount of energy represented by each α-cut$_i$. This fuzzy membership function is defined as follows:

$$\mu_3(\beta^{\mathrm{SMV}\perp}, i) := \frac{\| \vec{b}_i \|}{\| \vec{b}_0 \|}. \qquad (4.11)$$
$$1 \leq i \leq L$$

Then, FuzzyVD uses for the defuzzyfication process the following equations:

$$v(\alpha\text{-cut}_i) = \min(\mu_1, \mu_2) \times \mu_3. \qquad (4.12)$$

Therefore, FuzzyVD considers the α-cut$_i$ with the maximum valuation using (Equation 4.12) as the best way to induce a crisp partition, where the VD is the number of different classes in Γ_i.

$$\mathrm{VD}^{\mathrm{estimated}} = \#\Gamma_i, \qquad (4.13)$$

where the Γ_i is induced by the α-cut$_i$ with the maximum valuation using (Equation 4.12) and $1 \leq i \leq \#\Delta$.

4.2.1 Pseudo-Code

FuzzyVD algorithm

INPUT: X := Hyperspectral image.
INPUT: L := Dimensions number of X.
$\beta^{\text{SMV}\perp} = \text{SMV}\perp\,(X, L)$
$R_T \quad = CMER(X)$
$\Delta \quad = \text{Algorithm } \Delta(R_T, L)$
$\Gamma \quad = \text{Algorithm } \Gamma(R_T, \Delta, L)$
$\psi \quad = \text{Algorithm } \psi(\Gamma, L)$
$VD \quad = 0$
$max \quad = 0$
For $i = 1$ to $\#\Gamma$
  If $v(\Gamma, i) > max$
    $max = v(\Gamma, i)$
    $VD = \#\Gamma_i$
  End If
End For
OUTPUT: VD := Number estimated of endmembers in X.

This page is intentionally left blank.

Chapter 5

Experiments and Results

This chapter provides the steps used in this thesis to obtains the hyperspectral images used in the experiments, it describes the experiments performed, and it shows a comparative analysis of the results obtained by the proposed algorithms against related algorithms.

5.1 Hyperspectral Imagery Used in the Experiments

5.1.1 Synthetic Imagery

By recreating six synthetic hyperspectral images TI1, TI2, TI3, TE1, TE2 and TE3 as proposed Chein I. Chang in [16] as a base to test and compare algorithms for endmember extraction and VD estimation. Each image has 200×200 pixels, 224 bands from 0.4μm to 2.5μm, 25 panels created with five reflectance hyperspectral signatures: alunite (A: alunite_al706.966.asc [2]), buddingtonite (B: buddingtonite_gds85.3924.asc [2]), calcite (C: calcite_co2004.4113.asc [2]), kaolinite (K: kaolinite_cm3.11788.asc [2]), and muscovite (M: muscovite_gds107.14887.asc [2]) obtained from USGS [2]. The background is the mean of all spectral signatures. TI1, TI2, and TI3 are implanted panels where TI1 is noise free; TI2 has a background with Additive White Gaussian Noise ($AWGN$) SRN 20:1; TI3 has all pixels with $AWGN$ SRN 20:1. TE1, TE2, and TE3 are similar to TI1, TI2, and TI3 respectively but the panel pixels are embedded (signature + background).

For detailed instructions, please refer to [16].

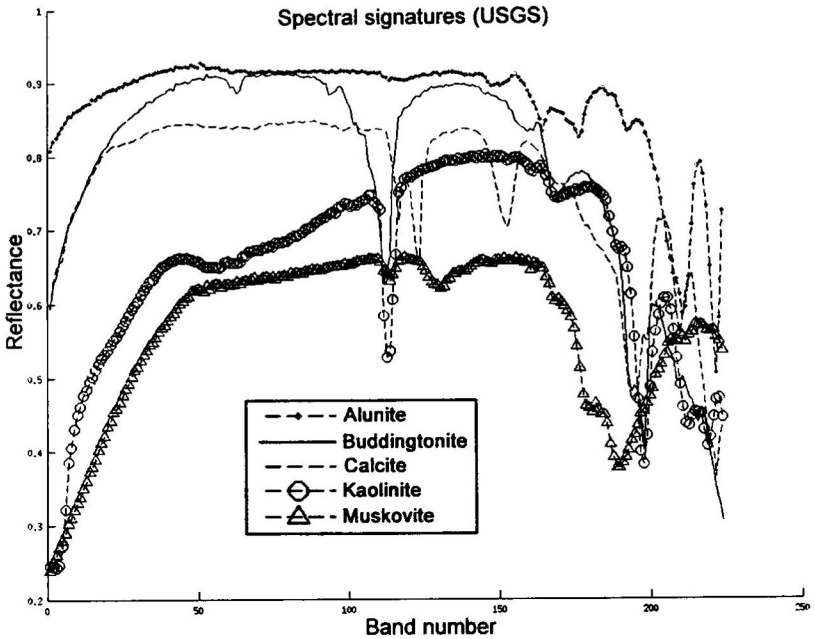

FIGURE 5.1: Five spectral signatures used in synthetic imagery.

The (Figure 5.1) shows the plot of each spectral signatures A, B, C, K, and M while the (Figure 5.2) shows the six synthetic hyperspectral images.

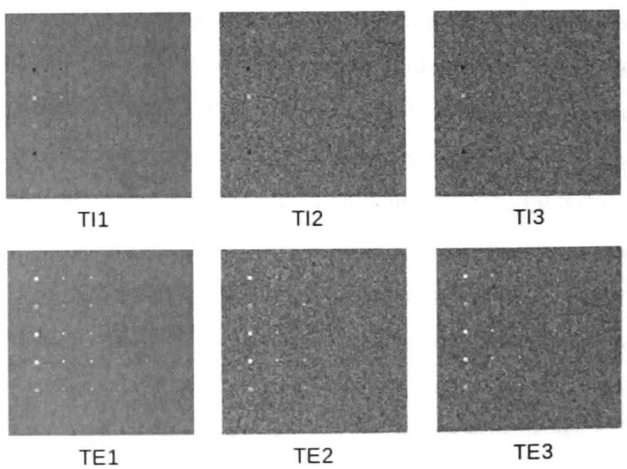

FIGURE 5.2: Band 1 in gray scale of each synthetic hyperspectral image created to be used in experiments.

5.1.2 Real AVIRIS Hyperspectral Images

One of the most used real HI for endmember extraction in the literature is the AVIRIS Cuprite, Nevada image available in [1].

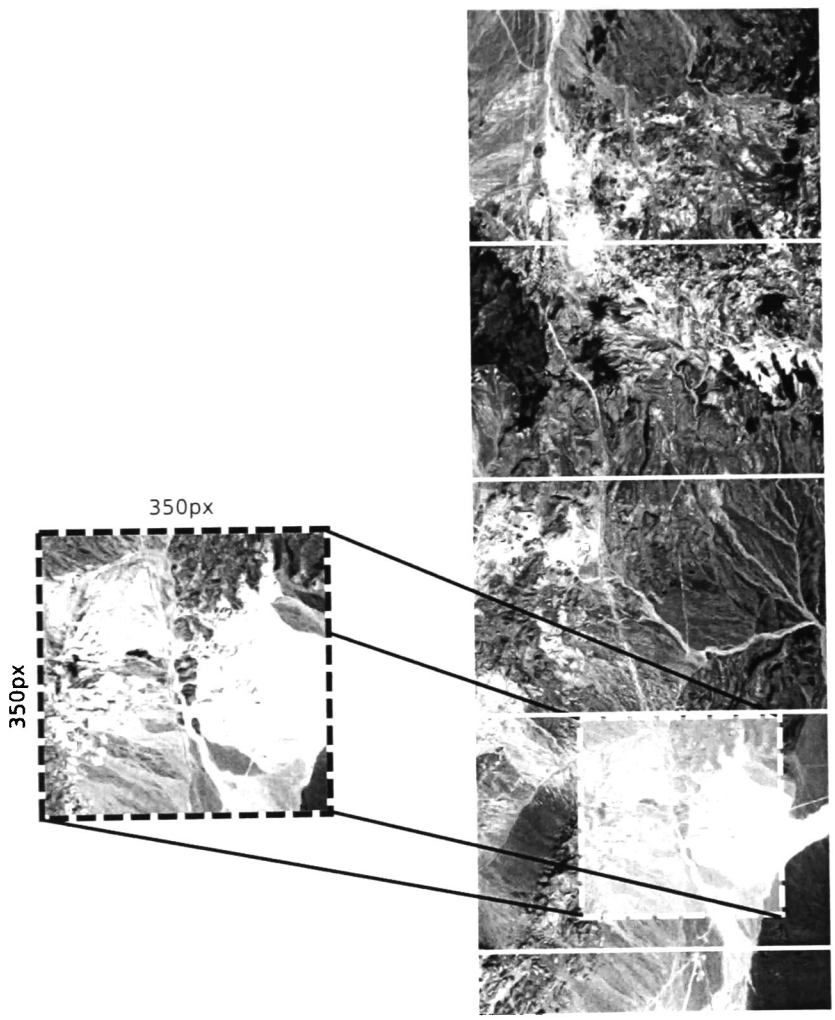

FIGURE 5.3: Original hyperspectral image from Cuprite, Nevada [1], remarking the area where was cut the sample used in experiments.

The (Figure 5.3) shows a representation of the full hyperspectral image provided by the AVIRIS project [1], it shows the area cut as a sample that was used in the experiments. This hyperspectral image was obtained in five parts, each of them has 615×512 pixels and 224 bands from $0.4\mu m$ to $2.5\mu m$. In the fourth part, there has been a cut sample of 350×350 pixels and 224 bands begging at row 1, column 263. The (Figure 5.4) shows

the resultant HI. Due to the fact that SMV⊥ does not requires dimensional reduction, band removal, or noise removal, all bands are present from the original image.

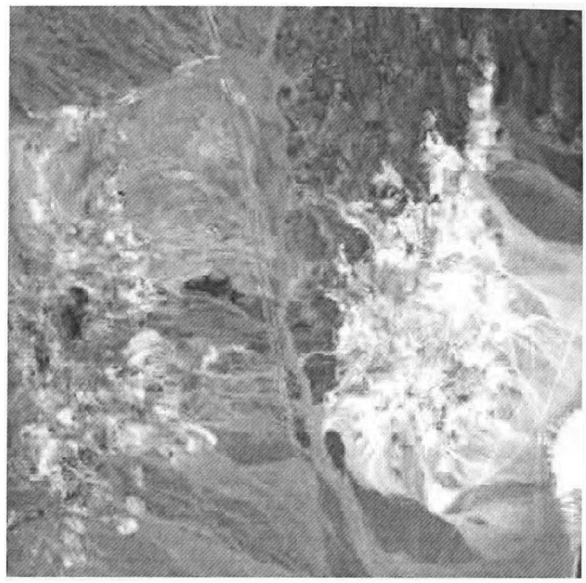

FIGURE 5.4: Real hyperspectral image from Cuprite, Nevada [1].

5.2 Experiment Descriptions

The SMV⊥ and FuzzyVD algorithms were compared against the more related algorithms present in the revised literature in order to measure their performance under the assumptions of the LMM.

5.2.1 SMV⊥

In this thesis, were used the N-FINDR and ATGP implementation provided by Chein I. Chang in [16], and all the algorithms were implemented in Matlab2010. The performance of SMV⊥, N-FINDR, ATGP and OBA were compared in reference to three measures: *number of arithmetic operations*, *empirical execution time*, and *volume of the simplex in* $\mathbb{R}^n$ The experiments were executed on a computer with the characteristics described in (Section 5.3.1.2).

5.2.2 FuzzyVD

In order to compare the results obtained with FuzzyVD, three other methods are used: HFC, NWHFC, and TEP. The implemented versions of HFC and NWHFC are from [16], the input parameters are the following:

$$P_F = \{10^{-1}, 10^{-2}, 10^{-3}, 10^{-4}, 10^{-5}\},$$

and TEP was implemented based on the normalized covariance eigenvalues, setting the input parameter $a\%$ as follows:

$$a\% = \{97\%, 98\%, 99\%, 99.5\%, 99.9\%\}.$$

All algorithms were applied to TI1, TI2, TI3, TE1, TE2, TE3, and Real AVIRIS.

5.3 Results

5.3.1 SMV⊥

5.3.1.1 Number of Arithmetic Operations

This measure is very important for algorithms performance evaluation because it provides a quantitative reference about the expected time consumed by the algorithms, and the computational complexity function behavior in reference to the input parameters variation. In the case of hyperspectral image analysis, the number of arithmetic operations is closely related with the number of spectral pixels, dimensions and the number of endmembers to be extracted.

The (Figure 5.5) shows the number of arithmetic operations performed by the SMV⊥ (Scale 1:1), N-FINDR (Scale 10:1), ATGP (Scale 10:1) and OBA (Scale 1:1) for synthetic imagery. All synthetic images have same number of pixels and dimensions; therefore, the number of arithmetic operations depends only on the number of endmembers to

extract. The range used in this thesis is 1,2,...,250. For N-FINDR, the number of arithmetic operation were calculated using the computational time complexity estimated in [31].

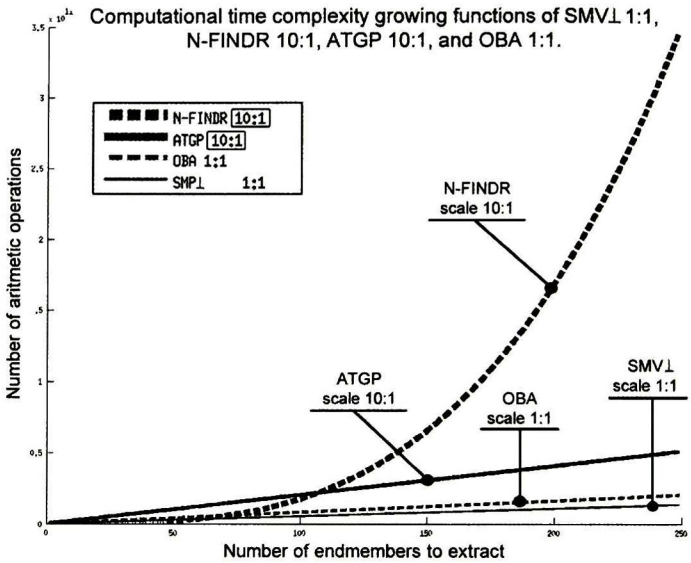

FIGURE 5.5: Number of arithmetic operations performed by SMV⊥, N-FINDR, ATGP, and OBA in reference to the number of endmembers to extract.

The (Figure 5.5) shows that SMV⊥ performs the fewest number of arithmetic operations.

5.3.1.2 Empirical Execution Time

The experiments were executed in a computer with the following characteristics:

1. Microprocessor Intel i5 1.70 GHz × 4.
2. 8GB RAM.
3. HDD 7200rpm.
4. Linux Ubuntu 14.04 LTS.
5. Matlab R2010b.

Due to the fact that N-FINDR depends on a random initialization process, the average time of 150 executions extracting 5 endmembers were registered during the experiments. For real AVIRIS images, the time is the fewer obtained after several executions. The (Table 5.1) shows the best execution times of the SMV⊥, N-FINDR, ATGP, and OBA algorithms.

	SMV⊥	OBA	ATGP	N-FINDR
TI1	0.57 s	0.92 s	1.13 s	23.72 s
TI2	0.54 s	0.93 s	1.15 s	38.05 s
TI3	0.54 s	0.93 s	1.17 s	35.61 s
TE1	0.54 s	0.87 s	1.16 s	41.14 s
TE2	0.54 s	0.83 s	1.17 s	20.22 s
TE3	0.55 s	0.91 s	1.15 s	32.62 s
AVIRIS	10.13 s	16.84 s	22.92 s	1,608.61 s

TABLE 5.1: Execution time extracting 5 endmembers in synthetic imagery and 29 endmembers in real AVIRIS image using SMV⊥, N-FINDR, ATGP, and OBA.

It is possible to observe in the (Table 5.1) that the faster algorithm in *empirical execution time* is SMV⊥. This result is congruent with the expected behavior.

5.3.1.3 Volumen of the Simplex in $\mathbb{R}^n$

The SMV⊥, N-FINDR, ATGP, and OBA algorithms search the set $E = \{\vec{e}_0, \vec{e}_1, ..., \vec{e}_{k-1}\}$ of vertices within the SMV^{k-1} Therefore, the algorithm with the best performance is capable to obtain the set E of maximum volume.

The (Figure 5.6) shows the *volume of the simplex in* $\mathbb{R}^n$ obtained by the SMV⊥, N-FINDR, ATGP, and OBA algorithms for synthetic and real HIs. For all hyperspectral images, the SMV⊥ algorithm obtained the simplex of maximum volume. Therefore, the volume of the simplex obtained by SMV⊥, N-FINDR, ATGP and OBA are expressed by the ratio:

$$\frac{\text{vol(SMV } \perp)}{\text{vol(SMV } \perp)},$$

$$\frac{\text{vol(N-FINDR)}}{\text{vol(SMV } \perp)}.$$

$$\frac{\text{vol(ATGP)}}{\text{vol(SMV}\perp)},$$

and

$$\frac{\text{vol(OBA)}}{\text{vol(SMV}\perp)}$$

respectively.

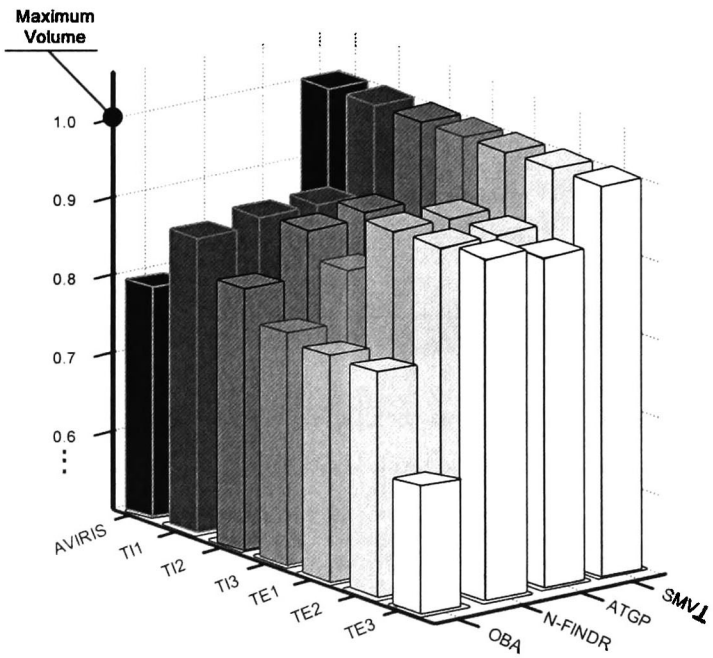

FIGURE 5.6: Volume obtained by the SMV⊥, N-FINDR, ATGP, and OBA algorithms applied to synthetic and real hyperspectral imagery.

The (Figure 5.6) allows to make the following remarks:

1. The algorithm capable to find the bigger volume is SMV⊥. In consequence, it is the algorithm with the best performance.

2. ATGP found a simplex with the volume grater or equal than N-FINDR and OBA.

3. The algorithm that found the smallest volume in all scenarios is OBA. Therefore, OBA showed the worst performance.

5.3.2 FuzzyVD

It is known in advance that 5 endmembers are present in each synthetic hyperspectral image. In the case of real AVIRIS image, there are, 27 possible. This number is due Chein I. Chang [16] who considers this number as a good estimation after band removal, noise removal and a $P_F = 10^{-3}$

In (Table 5.2), it is possible to see that FuzzyVD has obtained results similar to the desired output for synthetic hyperspectral images. However, only in the image TE2 estimation is completely correct. This may be due to the fact that the image is embedded and the total signal noise ratio is the lower of all synthetic hyperspectral images. The (Table 5.2) also shows that the VD estimated for real AVIRIS image is very similar in reference to the expected result.

FuzzyVD

	Synthetic Imagery						Real image
	TI1	TI2	TI3	TE1	TE2	TE3	AVIRIS
ideal	5	5	5	5	5	5	27
estimation	4	4	4	3	5	7	29

TABLE 5.2: VD estimated by FuzzyVD in synthetic real AVIRIS images.

The results of the HFC algorithm are shown in (Table 5.3). It is clear that the HFC performance is quite inferior to the proposed algorithm FuzzyVD. The hyperspectral images with better results are TI1 and TI2, but for the remainder hyperspectral imagery. The obtained results are unusable.

The (Table 5.4) shows the results for the NWHFC algorithm, they are similar to the ones in the table for HFC. It may be due to the fact that hyperspectral imagery used in this thesis does not remove any band. In addition, in the case of TE2 and AVIRIS, the HFC algorithm does not estimate the VD.

The (Table 5.5) shows the VD estimation based on eigenvalues. It is possible to see that this method provide a good performance when the endmembers do not have noise. This

HFC

P_F	*ideal*	10^{-1}	10^{-2}	10^{-3}	10^{-4}	10^{-5}
TI1	5	102	70	57	47	41
TI2	5	2	2	1	1	1
TI3	5	2	2	1	1	1
TE1	5	111	91	80	65	57
TE2	5	116	116	116	116	116
TE3	5	1	1	1	1	1
AVIRIS	27	99	61	49	44	36

TABLE 5.3: VD estimated using HFC in synthetic and real AVIRIS images.

NWHFC

P_F	*ideal*	10^{-1}	10^{-2}	10^{-3}	10^{-4}	10^{-5}
TI1	5	142	122	105	93	82
TI2	5	2	2	2	1	1
TI3	5	2	2	1	1	1
TE1	5	114	113	112	112	112
TE2	5					
TE3	5	1	1	1	1	1
AVIRIS	27					

TABLE 5.4: VD estimated using NWHFC in synthetic and real AVIRIS images.

is the case for TI1, but for the rest, the results are unusable.

Threshold Energy Percentage

a%	*ideal*	97%	98%	99%	99.5%	99.9%
TI1	5	3	3	4	4	4
TI2	5	217	219	222	223	224
TI3	5	217	219	222	223	224
TE1	5	1	1	1	2	4
TE2	5	1	1	1	1	1
TE3	5	215	218	221	223	224
AVIRIS	27	180	188	196	201	205

TABLE 5.5: VD estimated using Threshold Energy Percentage in synthetic and real AVIRIS images.

Chapter 6

Final Conclusions and Future Research

This chapter gives a conclusion and proposes the forthcoming research work.

6.1 Final Conclusions

This thesis proposes a novel idea to calculate the *simplex of maximal volume* in $\mathbb{R}^n$ for *linear mixing models* that can be used to reduce the complexity of the N-FINDR by implementing a bottom-up approach based in an observation from linear algebra and the exploitation of properties of the Gram-Schmidt algorithm. Therefore, the *Simplex of Maximal Volume Perpendicular* (SMV$\perp$) algorithm is proposed for fast endmember extraction in hyperspectral imagery. This novel algorithm has complexity $O(n)$ with respect to the number of pixels. SMV$\perp$ has been applied to hyperspectral image analysis and the evidence shows that SMV$\perp$ provides good performance because it obtains the simplex in $\mathbb{R}^n$ of maximal volume. In addition, it has lower computational time complexity than N-FINDR, ATGP, and OBA algorithms on synthetic and real AVIRIS images.

The estimation of the number of endmembers present in a hyperspectral image is a very important task because this number is an input parameter for many endmember

extraction algorithms. This thesis proposes a novel algorithm to estimate the number of endmembers present in a hyperspectral image by using fuzzy logic: the Fuzzy Virtual Dimensionality (FuzzyVD). Based on its results, this algorithm provides better performance than several of the classic algorithms often used to estimate the number of endmembers present in a hyperspectral image. Additionally, the FuzzyVD does not requires initial parameters. Furthermore, a new fuzzy system is proposed to deal with the selecting of the α-cut who generates the best partition. The evidence obtained allows to select the best α-cut for a fuzzy set when desired properties for the resultant crisp equivalence class are defined.

6.2 Future Research

1. Because there are publications [32] that describe successfully cases developing practical HSIs, this thesis proposes to develop a practical HIS in order to be able to acquire hyperspectral images to allow the application of the algorithms proposed in this thesis to practical applications of material detection, material identification, and material mapping.

2. Once developed the HSI, it is possible to use this to develop algorithms for target identification and discrimination, by exploring the capability to identify targets of interest in the hyperspectral dataset. Furthermore, it is interesting to use this HSI to propose new solutions for some open problems present in the literature of the computer vision, precision agriculture, industry, etc.

3. If it is possible to develop the target detection and identification by using the HSI developed, this thesis proposes to use the hyperspectral datasets acquired, to develop military application to identify cannabis fields, and clandestine laboratories, by mounting the HSI in drones, UAVs and airplanes.

Bibliography

[1] NASA. *AVIRIS Airborne Visible / Infrared Imaging Spectrometer.* Free AVIRIS Standard Data Products. United States of America. http://aviris.jpl.nasa.gov/data/free_data.html. Availabe January 2015.

[2] R. N. Clark, G. A. Swayze, R. Wise, K. E. Livo, T. M. Hoefen, R. F. Kokaly, and S. J. Sutley, 2007, USGS Digital Spectral Library splib06a, U.S. Geological Survey, Data Series 231.

[3] Telops. Obtained at March 20th, 2015, from http://www.telops.com/en/media-library/publications

[4] Alina Zare. *Hyperspectral endmember detection and band selection using Bayesian methods.* University of Florida, Florida, United States of America. 2008.

[5] Chein I. Chang and Qian Du. *Estimation of Number of Spectrally Distinct Signal Sources in Hyperspectral Imagery.* IEEE transactions on geoscience and remote sensing. March, 2004.

[6] Chein I. Chang, Wei Xiong, Hsian-Min Chen and Jyh-Wen Chai. *Maximum Orthogonal Subspace Projection Approach to Estimate the Number of Spectral Signal Sources in Hyperspectral Imagery.* Proc. Summer JPL Airborne Earth Science Workshop, Pasadena, CA. pp. 23-26 CA, 1995.

[7] Dimitris Manolakis and Gary Shaw. *Detection algorithms for Hyperspectral Imaging Applications.* IEEE Signal Processing Magazine January, 2002.

[8] Michael E. Winter. *N-FINDR: an algorithm for fast autonomous spectral end-member determination in hyperspectral data.* Part of the SPIE conference on Imaging Spectrometry V. Denver, Colorado. July, 1999.

[9] Chein I. Chang, Chao-Cheng Wu, Wei-min Liu and Yen-Chieh Ouyang. *A New Growing Method for Simplex-Based Endmember Extraction Algorithm.* IEEE Transactions on geoscience and remote sensing, Vol. 44, No. 10. October, 2006.

[10] J. W. Boardman, F.A. Kruse, and R.O. Green. *Mapping target signature via partial unmixing of AVIRIS data.* Proc. Summer JPL Airborne Earth Science Workshop, Pasadena, CA. pp. 23-26 CA, 1995.

[11] Xuetao Tao, Bin Wang and Liming Zhang. *Orthogonal Bases Approach for the Decomposition of Mixed Pixels in Hyperspectral Imagery.* IEEE Geoscience and Remote Sensing letters, Vol. 6, No. 2. April, 2009.

[12] Peter D. Lax. *Linear Algebra: Pure and Aapplied Mathematics.* New York, United States of America: John Wiley & Sons, Inc., 1997.

[13] Klaus Jänich. *Linear Algebra.* New York, United States of America: Springer-Velag. New York, United States of America. 1994.

[14] Chein I. Chang. *Exploration of Virtual Dimensionality in Hyperspectral Image Analysis.* Remote Sensing Signal and Image Processing Laboratory. Department of Computer Science and Electrical Engineering. University of Meryland, Baltimore Country, Baltimore. 2006.

[15] George J. Klir and Bo Yuang. *Fuzzy sets and fuzzy logic: theory and applications.* New Jersey, United States of America: Prentice Hall, 1995.

[16] Chein-I Chang. *Hyperspectral data processing: Algorithm design and analysis.* University of Maryland, Baltimore Country (UMBC), Maryland, United States of America. John Wiley & Sons, Inc., 2012.

[17] De Mauro, A., Greco, M., & Grimaldi, M. "What is big data? A consensual definition and a review of key research topics". In AIP Conference Proceedings (Vol. 1644, pp. 97-104). February, 2015.

[18] Xiaojin Zhu. "Semi-Supervised Learning Literature Survey" University of Wisconsin, Madison. December, 2007.

[19] Wei Xiong, Chein-I Chang, Chao-Cheng Wu, Konstantinos Kalpakis, and Hsian Min Chen. *Fast Algorithms to Implement N-FINDR for Hyperspectral Endmember*

Extraction. IEEE Journal of selected topics in applied earth observations and remote sensing. Vol. 4, No. 3. September, 2011.

[20] S. Chandrasekhar, *Radiative Transfer..* New York: Dover, 1960.

[21] Bioucas-Dias, J.M., Plaza, A., Dobigeon, N., Parente, M., Qian Du; Gader, P., and Chanussot, J., *Hyperspectral Unmixing Overview: Geometrical, Statistical, and Sparse Regression-Based Approaches.* Selected Topics in Applied Earth Observations and Remote Sensing, IEEE Journal Geoscience and Remote Sensing, vol.5, no.2, pp.354,379, April 2012.

[22] J. Plaza, A. Plaza, R. Perez, and P. Martinez, "On the use of small training sets for neural network-based characterization of mixed pixels in remotely sensed hyperspectral images," Pattern Recognition, vol. 42, pp. 3032–3045, 2009.

[23] G. Licciardi and F. Del Frate, "Pixel unmixing in hyperspectral data by means of neural networks," IEEE Trans. Geosci. and Remote Sens., vol. 49, no. 11, pp. 4163 –4172, nov. 2011.

[24] K. J. Guilfoyle, M. L. Althouse, and C.-I. Chang, "A quantitative and comparative analysis of linear and nonlinear spectral mixture models using radial basis function neural networks" IEEE Trans. Geosci. and Remote Sens., vol. 39, no. 8, pp. 2314–2318, Aug. 2001.

[25] R. Close, P. Gader, and J. Wilson, "Hyperspectral endmember and proportion estimation using macroscopic and microscopic mixture models," IEEE Trans. Geosci. and Remote Sens., 2012, in preparation.

[26] J. M. P. Nascimento and J. M. Bioucas-Dias, "Vertex component analysis: A fast algorithm to unmix hyperspectral data," IEEE Trans. Geosci. and Remote Sens., vol. 43, no. 4, pp. 898–910, 2005.

[27] J. Gruninger, A. Ratkowski, and M. Hoke, "The sequential maximum angle convex cone (SMACC) endmember model" in Proc. SPIE, vol. 5425, 2004, pp. 1–14.

[28] Green, A.A., M. Berman, P. Switzer, and M.D. Craig. *A Transform for Ordering Multispectral Data in termsof Image Quality with Implications for Noise Removal.* IEEE Trans. Geosci. Remote Sens. Vol 26, NO. 1, pp. 65-74. 1988.

[29] Bing Xu and Peng Gong. *Noise estimation in a noise-adjusted principal component transformation and hyperspectral image restoration.* Can. J. Remote Sensing. Vol 34, NO. 3, pp. 271-286. 2008.

[30] Raúl Ramírez Ramírez. *Introducción al Análisis de Componente Principal y al Análisis de Componentes Independiente usando Scilab.* Instituto Politécnico Nacional (IPN UPIITA). México D.F. Summer 2008.

[31] Junmin Liu and Jiangshe Zhang. *A New Maximim Simplex Volume Method Based on Housholder Transformation for Endmember Extraction.* IEEE Transactions on geoscience and remote sensing, Vol. 50. No. 1. January, 2012.

[32] Ralf Habel, Michael Kudenov and Michael Wimmer. "Practical Spectral Photography". EUROGRAPHICS 2012 / P. Cignoni, T. Ertl. Volume 31, Number 2. 2012.

[33] Jairo Salazar-Vazquez and Andres Mendez-Vazquez. *FuzzyVD: An algorithm that uses Fuzzy Logic and Fuzzy Systems to estimate the number of endmembers present in a hyperspectral image.* Centro de Investigación y Estudios Avanzados del Insituto Pilitécnico Nacional, Campus Guadalajara. NAFIPS'2015. Seattle, Washington, USA. 2015.

[34] Rawlings, John O., Pantula, Sastry G., Dickey, David A. *Applied Regression Analysis: A Research Tool.* Wadsworth & Brooks, Pacific Grove. 1989.

[35] José M. Bioucas-Dias and José M.P. Nascimento. *Hyperspectral Subspace Identification.* IEEE Transactions on geoscience and remote sensing. Vol 46, NO. 8. August, 2008.

[36] R. E. Roger and J. F. Arnold. *Reliability estimating the noise in AVIRIS hyperspectral images.* Int. J. Remote Sensing, vol. 17, no. 10, pp.1951 -1962 1996.

[37] Jairo Salazar-Vazquez and Andres Mendez-Vazquez. *SMV⊥: An algorithm to calculate the simplex of maximal volume in $\mathbb{R}^n$ based upon Gram-Schmith process.* Centro de Investigación y Estudios Avanzados del Insituto Pilitécnico Nacional, Campus Guadalajara. SPIE, Remote Sensing. Toulouse, France. 2015.

CENTRO DE INVESTIGACIÓN Y DE ESTUDIOS AVANZADOS DEL I.P.N.
UNIDAD GUADALAJARA

El Jurado designado por la Unidad Guadalajara del Centro de Investigación y de Estudios Avanzados del Instituto Politécnico Nacional aprobó la tesis

Extracción automática de pixeles puros para el análisis de imágenes hiperespectrales. / Automatic endmember extraction algorithms for hyperspectral image analysis

del (la) C.

Jairo SALAZAR VÁZQUEZ

el día 28 de Agosto de 2015.

Dr. Luis Ernesto López Mellado
Investigador CINVESTAV 3C
CINVESTAV Unidad Guadalajara

Dr. Federico Sandoval Ibarra
Investigador CINVESTAV 3C
CINVESTAV Unidad Guadalajara

Dra. Susana Ortega Cisneros
Investigador CINVESTAV 3A
CINVESTAV Unidad Guadalajara

Dr. Andrés Méndez Vázquez
Investigador CINVESTAV Guadalajara 2C
CINVESTAV Guadalajara